



Science & Global Security

The Technical Basis for Arms Control, Disarmament, and Nonproliferation Initiatives

ISSN: (Print) (Online) Journal homepage: www.tandfonline.com/journals/gsgs20

Hypersonic Cruise Missiles

David Wright & Cameron L. Tracy

To cite this article: David Wright & Cameron L. Tracy (08 Jan 2025): Hypersonic Cruise Missiles, Science & Global Security, DOI: [10.1080/08929882.2024.2447176](https://doi.org/10.1080/08929882.2024.2447176)

To link to this article: <https://doi.org/10.1080/08929882.2024.2447176>



Published online: 08 Jan 2025.



Submit your article to this journal 



View related articles 



View Crossmark data 



Hypersonic Cruise Missiles

David Wright^a and Cameron L. Tracy^{b*} 

^aLaboratory for Nuclear Security and Policy, Department of Nuclear Science and Engineering, MIT, Cambridge, MA, USA; ^bCenter for International Security and Cooperation (CISAC), Freeman Spogli Institute for International Studies, Stanford University, Stanford, CA, USA

ABSTRACT

This paper analyzes hypersonic cruise missiles (HCMs) powered by hydrocarbon-fueled scramjets and compares their capabilities to other systems that might perform the same missions, including hypersonic boost-glide vehicles (BGVs) and maneuverable reentry vehicles (MaRVs). Most analysis of hypersonic weapon capabilities has focused on BGVs, while HCMs are a distinct technology with distinct characteristics. We analytically model the X-51A HCM vehicle that the United States flight tested in 2010–13 and use that model as a basis for assessing the potential performance of near-term HCMs for military use. We find that these HCMs can have lower masses than BGVs of the same maximum range, but significantly higher masses than MaRVs of the same range. Because these HCMs use hydrocarbon fuels, they are limited to flying at low hypersonic speeds relative to BGVs and MaRVs, giving them longer flight times than those systems over the same range and making them vulnerable to interception by terminal missile defenses. We find that HCMs can be more maneuverable than BGVs during the atmospheric portion of their flight, though less maneuverable than supersonic cruise missiles.

ARTICLE HISTORY

Received 20 August 2024
Accepted 28 November 2024

Introduction

Hypersonic missiles are weapons that travel faster than Mach 5, or five times the speed of sound. Hypersonic cruise missiles (HCMs) are hypersonic weapons that carry fuel and engines to power them for much of their flight through the atmosphere at low altitudes. This contrasts with hypersonic boost-glide vehicles (BGVs), which glide without power after being accelerated to hypersonic speeds by rocket boosters.¹

In two previous papers, we analyzed the performance of BGVs and compared their capabilities to those of alternative missile technologies that might carry out the same missions: maneuvering reentry vehicles (MaRVs)

CONTACT David Wright  dcw654@gmail.com  Laboratory for Nuclear Security and Policy, Department of Nuclear Science and Engineering, MIT, 2 Windermere Lane, Arlington, MA 02476, USA.

*Present address: Berkeley Risk and Security Lab, University of California, Berkeley, USA.

© 2025 Taylor & Francis Group, LLC

launched on ballistic missiles flying on depressed trajectories.² In this paper, we continue that analysis and comparison to include HCMs.

HCMs are powered by airbreathing engines called scramjets. Scramjets burn fuel the vehicle carries using oxygen from the atmosphere, which means they do not need to carry an oxidizer onboard as rockets do, reducing the mass they need to carry. However, scramjets can only operate at speeds greater than about Mach 4. They must therefore be accelerated to near-hypersonic speeds by some other method, such as a rocket booster, before the scramjet engine can start. Scramjets of the type used for HCMs can operate only up to speeds of Mach 7 to 8, which is less than the speeds at which many long-range BGVs typically fly.

Several countries, including the United States, Russia, and China are developing HCMs. Reports of Russia and China fielding versions of these weapons in recent years appears to have heightened interest among U.S. policymakers and defense officials in developing similar weapons at a rapid pace, but without a clearly articulated mission for these weapons or assessment of their utility, at least in the public realm.

It is not surprising that countries are interested in researching this technology. However, it is important to assess the capability of these systems relative to alternatives, and assess whether rapid fielding is justified, not only to ensure efficient use of resources, but because developing and fielding weapons based on unclear or exaggerated understandings of their capabilities can reduce international security by increasing threat perceptions between countries while providing little military benefit.

Current developments

HCMs have an intuitive appeal because adding an engine to a hypersonic vehicle would help it to overcome the drag forces encountered during low-altitude flight, which greatly slow BGVs throughout their trajectories, and could therefore keep the vehicle at a constant speed when the engine is burning. On the other hand, as we discuss below, adding an engine complicates the vehicle's operation in some important ways.

The U.S. military is currently interested in developing HCMs with low mass that can be launched from aircraft.³ In particular, the U.S. Air Force is developing an HCM as a potential alternative to air-launched boost-glide vehicles, like the Air-launched Rapid Response Weapon (ARRW).⁴ In addition, the Navy has started the Hypersonic Air Launched Offensive Anti-Surface Warfare (HALO) program to develop an air-launched weapon for its F/A-18 fighter aircraft, although recent reports say this system will probably fly at supersonic rather than hypersonic speeds.⁵

A current goal is to carry HCMs on combat aircraft like the F-35 rather than only large bombers like the B-52. This requires keeping their mass

below about 2,300 kg (5,000 lb) since the F-35 has two external pylons for carrying ordinance up to 2,300 kg.⁶ (Reports suggest that the F-15EX will have an external pylon that can carry about 3,200 kg on the aircraft's centerline, and the new external pylon on the B-1 may carry up to 3,400 kg.)⁷ ARRW with its booster is reported to have a mass of about 2,300 kg, so it could apparently also be carried on the F-35.⁸

The primary U.S. HCM currently in development is the air-launched Hypersonic Attack Cruise Missile (HACM). A recent report by the U.S. Congressional Budget Office estimates that the HACM would have a range of about 500 km.⁹ This system has become a higher priority recently because of problems seen in the ARRW testing program, which has led to delays and possible cancelation of that missile.¹⁰

In addition, the Air Force Research Laboratory is reportedly developing a larger, multi-purpose HCM vehicle called Hypersonic Multi-mission ISR and Strike, nicknamed Mayhem.¹¹ Little is known publicly about this program, but it is reportedly larger than HACM and is designed to carry sensors for surveillance or various types of warheads for strike missions. It is intended to be air-launched, but reports suggest its mass could be up to about 3,200 kg.¹² Recent reports state that funding for the project has been cut and the Air Force is exploring alternatives for these missions.¹³

Russia has fielded a ship-launched HCM (Zircon), which reportedly has a range of about 400 km flying at Mach 5 to 6, and can be fired from surface ships, submarines, and ground-based launchers.¹⁴ Zircon may first have been used in early 2024.¹⁵ China claims to have tested an HCM in 2018, the Starry Sky II, using a ground-based booster for the test launch. It reportedly has a range of 700 to 800 km with a top speed of Mach 6.¹⁶ Few details are known about these systems.

Key issues

The goal of this paper is to analyze the capabilities of HCMs and compare them to other hypersonic systems. Because more information is available about U.S. systems than Russian and Chinese systems, our assessment is based on an analysis of HCMs the United States has developed and tested for military applications, and extensions of the technology used in those systems.

Key issues for air-launched systems are missile mass, flight speed, range, and maneuverability. As mentioned above, the mass of HCMs is an important parameter because of the interest in carrying them on various aircraft. The mass an aircraft must carry is the combined mass of the hypersonic vehicle and its rocket booster; we call this the total mass of the system, M_{tot} .

One major difference in total mass between an HCM and a BGV comes from the mass of the booster needed for these two vehicles, which is related to the velocity to which the booster must accelerate them at the beginning of their flight. To achieve the same range, a BGV must be boosted to a higher initial speed than an HCM since the BGV slows due to drag as it glides, while the HCM burns fuel to maintain a constant speed. Since booster mass increases roughly exponentially with its top speed, if the BGV and HCM vehicles have similar masses, then the total mass of the BGV of the same range will generally be significantly larger.¹⁷ Similarly, a MaRV of similar mass requires a higher initial speed than an HCM, and thus a heavier booster, to reach a given range.

However, the total mass also scales with the vehicle mass, so if a BGV or MaRV vehicle can be made less massive than an HCM, which must carry fuel as well as the scramjet engine and its related technical systems, then the mass advantage of the HCM might disappear.

A second important issue is that the HCMs currently being developed are limited to speeds in the low hypersonic range, up to only about Mach 7, as discussed below. This is an intrinsic limitation of using hydrocarbon fuels—essentially types of jet fuel—rather than cryogenic fuels like hydrogen that can give higher speeds but are less suited to military uses.

These relatively low speeds mean HCMs might have longer flight times than BGVS and MaRVs. They will also not be fast enough to be evade current terminal missile defense systems, such as the PAC-3 MSE, which requires speeds of Mach 9 to 10 when the weapon begins its dive toward its target.¹⁸ These weapons would therefore not be suited to attacking missile defenses early in a conflict, which is an important mission the U.S. military sees for hypersonic weapons, as well as concern about the capabilities of adversaries.¹⁹

This paper analyzes the performance of air-launched HCMs. Much of this analysis is based on the design of the X-51A vehicle that the United States tested several times in 2010–13, which we show is a good model for the HCMs the United States is currently developing. In particular, we:

- Develop an approximate model of the X-51A vehicle based on published information about the X-51A program and its flight tests, quantifying a set of parameters to represent the general properties and capabilities of an X-51A-like vehicle.
- Vary the parameters of the X-51A model to assess how the capabilities of such a vehicle would change with hypothetical advances in HCM technology.
- Analyze the tradeoff between maneuvering and range of an X-51A-like HCM.

- Compare the range and flight-time capabilities of an X-51A-like HCM with those of BGVs and MaRVs having the same total mass.

We find that the HCMs we consider have lower masses than BGVs of the same maximum range but have higher masses than MaRVs. We show that because HCMs being developed for military missions use hydrocarbon fuels, they are limited to flying at low hypersonic speeds relative to BGVs and MaRVs, giving them longer flight times than those systems over the same range and making them vulnerable to interception by terminal missile defenses. We find that HCMs can be more maneuverable than BGVs during their midcourse phase of flight, but not as maneuverable as supersonic vehicles.

Scramjet engines

A typical jet engine combines fuel and air in a combustion chamber at high pressure, then uses the energy released by the resulting chemical reaction to accelerate its combustion products to high speed. This increase in the velocity of the exhaust relative to the speed of the air entering the engine creates thrust to propel the vehicle attached to the engine.

A turbojet uses a fan to actively pump air into the combustion chamber and increase the pressure in the chamber before the fuel-air mixture ignites, enhancing the thrust produced. If the vehicle is traveling fast enough, above about Mach 3, the motion of the vehicle through the atmosphere compresses the air as it is slowed to subsonic speeds while entering the combustion chamber, so that no turbofan is needed; such engines are called ramjets. At even higher speeds, above Mach 4 to 5, the air entering the combustion chamber is traveling fast enough that it cannot be brought to subsonic speeds without raising the temperature so much that it dissociates the fuel and limits the energy added by combustion.²⁰ Instead, in scramjet (supersonic-combustion ramjet) designs, the air is slowed somewhat to increase the pressure but still flows through the combustor at supersonic speeds while the fuel ignites (see [Figure 1](#)).

This process can produce significant thrust, but also raises engineering challenges. For example, for a scramjet with a combustion chamber less than a meter in length, like the X-51A has, the residence time of air in the combustor is less than a millisecond, during which time the air and the fuel must mix efficiently, ignite, and complete their burn. Moreover, the turbulent flow of air into the engine must remain steady enough to keep the reaction going. This process has been compared to “lighting a match in a hurricane and keeping it burning.”²¹

In addition, as the vehicle’s speed increases, the kinetic energy of the incoming air increases relative to the energy released in the chemical

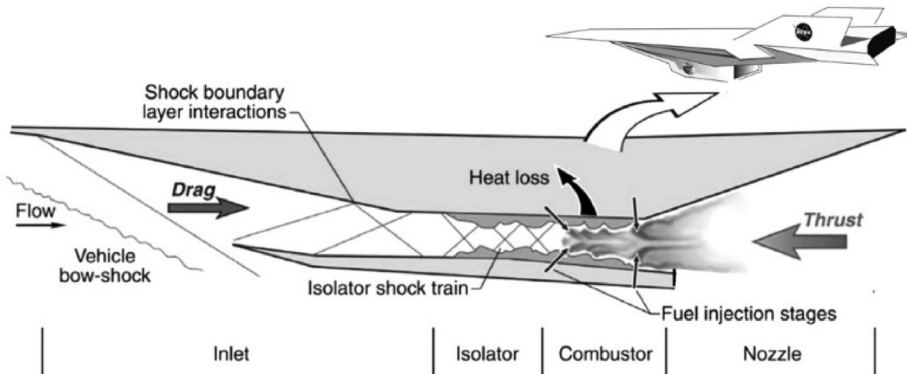


Figure 1. A schematic cross-section of a scramjet engine, showing the air inlet on the left and exhaust ejection on the right. In the diagram of the X-43A at the top right, the scramjet engine is the object on the lower surface of the vehicle (Source: Modified from <https://www.nasa.gov/reference/x-43a/>).

reaction, so that the thrust produced by the engine decreases roughly inversely to the vehicle's velocity.²² Above speeds of Mach 7 to 8, the energy output of hydrocarbon fuels is too low to produce useful thrust and a fuel like hydrogen is required. Hydrogen releases nearly three times the energy per unit mass of jet fuels and has very short ignition and burn times. However, it is much less dense than jet fuel, requiring a larger volume of hydrogen to provide the same amount of energy. The larger volume required for fuel storage on a hydrogen-fueled vehicle leads to higher drag, which can make it difficult for the vehicle to achieve a high thrust-to-drag ratio.²³ In addition, storage is more difficult since hydrogen must be kept at high pressures or low temperatures, unlike hydrocarbon fuels.

The details of scramjet operation also limit the trajectories that HCMs can fly. While air-breathing engines do not need to carry the extra mass of onboard oxidizer as a rocket engine does, they must intake sufficient air during flight, limiting their ability to fly at high altitudes where the air is less dense.

HCMs circulate the fuel they carry throughout the vehicle to absorb heat and actively cool parts of the engine and vehicle surface, which both reduces the heat loads on the vehicle and preheats the fuel, improving combustion. The vehicle must be designed so that the amount and flow rate of fuel is matched to the speed and altitude at which the vehicle will be flown, which affects its heating.

These are examples of the difficulties of designing and operating HCMs due to the tight coupling between the design of the vehicle and its speed, flight altitude, and range on the intended trajectory. The vehicle must be designed to generate sufficient lift to keep itself aloft while generating low drag to maintain its flight speed, giving a high lift-to-drag ratio (L/D); to

collect sufficient airflow for the engine; to withstand the mechanical stress and heating of hypersonic flight; and to carry enough fuel to reach the desired range, all while keeping the vehicle mass acceptably low.

Many aspects of HCM design are considerably more complicated than designing and flying a BGV. BGVs can be designed to have high L/D and be flown at a dynamic pressure and angle-of-attack chosen to maximize L/D . In contrast, while the scramjet is operating, an HCM must be flown at high dynamic pressure and small angle-of-attack (see [Appendix A](#)). Modeling HCM flight then requires knowing how lift and drag vary with angle-of-attack.

Ground testing of hypersonic systems is challenging because ground facilities, such as wind tunnels, cannot create high fidelity simulations of all the important aspects of extended hypersonic flight.²⁴ As a result, while research and development of scramjet engines and vehicles powered by them has been underway for decades, developing a practical vehicle using a scramjet engine has proved difficult.

The X-51 and X43 programs

The United States conducted flight tests of two HCMs between 2004 and 2013: the X-43A, which was fueled with hydrogen, and the X-51A, which used hydrocarbon fuel. Both were air-launched using rocket boosters released from B-52 aircraft.

The X-43A was twice as heavy as the X-51A and had large lifting surfaces compared to the more streamlined X-51A, which used a waverider design that uses its shock wave to increase vehicle lift.²⁵ In two tests in 2004, the X-43A flew at altitudes near 30 km, cruising at speeds of Mach 6.83 and Mach 9.68. The scramjet operated for 10 to 11 seconds in both cases, burning one to two kilograms of hydrogen.²⁶

In contrast, in 2013 the X-51A flew at altitudes near 20 km at a speed of about Mach 5, and its engine burned 120 kg of JP-7 fuel over three and a half minutes. [Figure 2](#) shows a schematic of the X-51A vehicle with its booster and the interstage section that connects them.

While the X-51A was a research vehicle, it was also viewed as a prototype for an HCM weapon, being roughly the right size and capability. Its designers stated that the test platform was “primarily a technology demonstrator vehicle but could quickly be adapted to an operational hypersonic cruise missile application.”²⁷ The Chief Scientist of the U.S. Air Force during much of the vehicle’s development wrote that “The X-51 vehicles are full scale and can be seen as leading directly to a high-speed weapon system.”²⁸

In addition, the Air Force’s program manager for the system stated that the X-51 served as the model for an HCM design, the High-Speed Strike

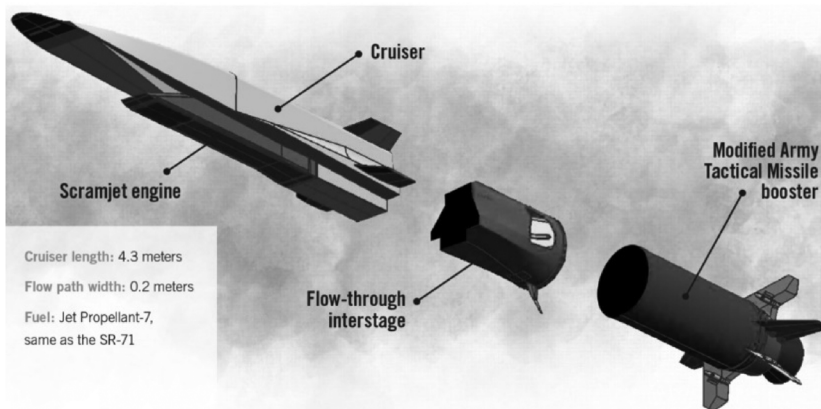


Figure 2. A schematic of the X-51A vehicle (left) with its booster (right) and the interstage section that connects them (Source: <https://aerospaceamerica.aiaa.org/features/scaling-up/>).

Weapon (HSSW), compatible with both B-2A and F-35 aircraft, and that “We foresee scramjet technology could be brought to bear to propel a light vehicle like X-51 in size anywhere between Mach 5 and 6 against targets 500 to 600 nm [900–1100 km] away within 10–12 min.”²⁹

The HSSW program was started around 2013 to develop a weapon based on the X-51A; within a few years it was replaced by the Hypersonic Air-breathing Weapon Concept (HAWC) program. HAWC was a joint Defense Advanced Research Projects Agency (DARPA) and Air Force program that had four successful flight tests in 2021–3 before the program ended. During its second flight test, in March 2022, HAWC’s scramjet reportedly burned for 327 seconds compared to 210 seconds for the longest X-51A burn.³⁰ This implies it carried nearly 190 kg of fuel, assuming the fuel consumption rate was similar to that of the X-51A.

HAWC was followed by the MOHAWC program, intended to further develop HAWC technology and contribute to the HACM program, which is currently the main hypersonic focus of the Air Force.

Few details are publicly available about HAWC and HACM. However, reports say that HACM’s airframe and engine designs are “very close” to those of HAWC,³¹ which grew out of the X-51A and HSSW programs, and that HACM is smaller than ARRW, which weighs about 2,300 kg with its booster, giving it a mass similar to the X-51A (see below). In addition, HACM is estimated to have an intended range of about 500 km, which is similar to but slightly longer than the X-51A (see range estimates in Table 1).³²

For these reasons, considering modified versions of the X-51A vehicle appears to be a reasonable approach to understanding the capabilities of systems like HACM that are currently being developed.

Analysis of the X-51A vehicle and 2013 flight test

Reports about the 1 May 2013 final flight test of the X-51A give the following information about the test.³³

A B-52H bomber released the stack (X-51A vehicle and booster) at an altitude of 40,000–50,000 ft (12.2–15.2 km) and speed of Mach 0.8 (240 m/s). The stack fell for 4 s from the B-52 before the rocket booster, a modified Army Tactical Missile System (ATACM) motor, ignited. The booster burned for 26–29 s, traveling about 25 km and reaching 63,000 ft (19.2 km) and Mach 4.9 (1,446 m/s), before it released the X-51A vehicle.³⁴

The process to start the X-51A vehicle's engine began before it separated from the rocket booster, initially burning ethylene and then transitioning to JP-7 fuel. Full power started 10–15 s after separation.³⁵ During this time the vehicle slowed somewhat and dropped to slightly lower altitude, with powered flight starting at Mach 4.83 (1,425 m/s).³⁶

The vehicle flew at essentially constant dynamic pressure q_0 , in the range 105–113 kPa.³⁷ If the lower value corresponds to the start of the full-power phase of flight, it implies that phase started at an altitude of about 62,500 ft (19.1 km). The scramjet burned JP-7 fuel for 209–212 s until it ran out of fuel, which occurred at an altitude of 63,500 ft (19.4 km) and speed of Mach 5.1 (1,505 m/s).³⁸

After the powered phase ended, the operators conducted maneuvers of the vehicle while it descended and dropped into the ocean.³⁹ The vehicle reportedly traveled 340 nm (630 km) from the point it was released from the B-52, with a total flight time of about nine minutes, which included about five minutes of descent.⁴⁰ The duration of “controlled flight,” presumably before operators lost contact with the vehicle during its descent, was reported to be 361 s.⁴¹ Telemetry was reported lost at an altitude of 20,000 ft (6.1 km).⁴²

Estimating the lift and drag coefficients

We use this information to estimate the X-51A's lift and drag coefficients C_L and C_D as functions of angle-of-attack α . The values that enter the calculations below are the products C_LA and C_DA , where A is a reference area for the vehicle.⁴³

A key parameter for HCM flight is the dynamic pressure, defined as:

$$q_0 = \frac{1}{2} \rho V^2 \quad (1)$$

where ρ is the atmospheric density and V is the vehicle's velocity. Dynamic pressure characterizes the kinetic energy per unit volume of the air surrounding a vehicle.

HCMs are flown at large values of q_0 to achieve sufficient engine air flow. The thrust of the scramjet is proportional to the rate of mass flow of air (\dot{m}_a) through the engine, which determines the rate at which the engine can burn fuel. The mass flow of air can be written in terms of q_0 as:

$$\dot{m}_a = \frac{2q_0 A_{in}}{V} \quad (2)$$

where A_{in} is the air inlet capture area that the vehicle uses to get air to the engine (see [Appendix A](#)).⁴⁴ Large \dot{m}_a therefore requires a large q_0 .

At the same time, q_0 must be kept low enough that it does not lead to excessive heating and mechanical stress on the vehicle. The mechanical forces on the vehicle are proportional to $\rho V^2 \sim q_0$, and the aerodynamic heating rate scales roughly as $\rho V^3 \sim q_0 V$.

These limitations on q_0 restrict sustained flight for scramjets to a relatively small range of combinations of altitude and velocity.⁴⁵ The value of q_0 is kept relatively constant during flight to maintain high thrust and acceptable levels of mechanical stress and heating (see [Appendix A](#)).

The data from the end of powered flight of the final X-51A flight test ($V = 1,505 \text{ m/s}$ and altitude 63.5 kft (19.4 km)) give $q_0 = 110 \text{ kPa}$ at that point. We assume from above that $q_0 = 105 \text{ kPa}$ at the beginning of powered flight, and below use an average value of 107.5 kPa during powered flight in our calculations.

Lift coefficient

For the vehicle to remain aloft the lift force F_{lift} must offset the gravitational force:

$$F_{lift} = \frac{1}{2} C_L A \rho V^2 = C_L A q_0 = M(t) g \lambda \quad (3)$$

where the second equality uses [Equation 1](#), $M(t)$ is the vehicle's mass at time t , $g = 9.8 \text{ m/s}^2$, and

$$\lambda(V) = 1 - \frac{V^2}{V_e^2} \quad (4)$$

is an inertial term that reduces the gravitational force due to the high speed of the vehicle. Here $V_e = [g(R_e + h)]^{1/2}$ is the orbital speed of an object at an altitude h ; $V_e \approx 7,915 \text{ m/s}$ at altitudes considered here. $\lambda(V)$ varies slowly with V in the range of speeds considered here, from 0.965 at Mach 5 to 0.932 at Mach 7.

[Equation 3](#) gives:

$$C_L A = \frac{M g \lambda}{q_0} \quad (5)$$

which determines the value of the lift coefficient needed to keep the vehicle aloft. The atmospheric density (and therefore the flight altitude) at any point in the vehicle's trajectory can be found from:

$$\rho = \frac{2q_0}{V^2} = \frac{2Mg\lambda}{C_L A V^2} \quad (6)$$

Since q_0 remains nearly constant during flight, the vehicle will vary its angle-of-attack to change the lift coefficient during powered flight since the vehicle mass changes as the propellant burns.⁴⁶

The launch mass of the X-51A was reported as 683 kg and its mass after scramjet burnout was apparently 557 kg. The mass of "usable JP-7" fuel was 120 kg (265 lb). The 126 kg (277 lb) difference between the launch and operating masses presumably includes the ethylene used to start the combustion of JP-7 in the scramjet. The total mass of the vehicle, booster, and interstage was 1,790 kg, of which 73 kg was the interstage and 6 kg was ethylene used to start the scramjet.⁴⁷

In the following analysis, we assume that during the powered phase (when the scramjet is operating) the vehicle burns 120 kg of JP-7 fuel in a time $t_b = 210$ s, for a fuel flow rate $\dot{m}_f = 0.57$ kg/s, and during this time its mass goes from $M_0 = 677$ kg (the launch mass minus the mass of ethylene burned prior to scramjet operation) to $M_f = 557$ kg.

Equation 5 then gives the lift coefficient $(C_L A)_0 = 0.061 m^2$ at the beginning of powered flight and $(C_L A)_f = 0.048 m^2$ at the end. This means the vehicle will fly with a somewhat larger angle-of-attack α at the beginning than the end of powered flight; we show below that this change in α is less than a degree.⁴⁸

Drag coefficient

The drag force on the vehicle is:

$$F_{drag} = \frac{1}{2} C_D A \rho V^2 = C_D A q_0 \quad (7)$$

Below we estimate the value of L/D that the vehicle demonstrates during its glide phase after powered flight has ended. Since the glide range is proportional to L/D we assume that the vehicle would glide at an angle of attack that maximizes L/D .

However, during powered flight the vehicle will typically not fly at maximum L/D . As noted above, to generate high thrust the vehicle will

fly at high q_0 (high velocity at low altitude) to increase the air flow to the engine, and [Equation 3](#) for the lift force at constant altitude flight will require a value of α smaller than the value that maximizes L/D . Having small values of drag near that value of α is important for increasing the net thrust (the difference between the thrust provided by the engine and the drag force) during powered flight.⁴⁹

To determine the drag of the vehicle, we therefore estimate the variation of the lift and drag coefficients with α by fitting to data from the 2013 test, as follows.

Reports state that the X-43A hypersonic vehicle flew at angle-of-attack $\alpha=1$ to 2.5 degrees during its powered phase,⁵⁰ and we therefore assume the X-51A also flew at small angles. For small α we assume the lift and drag coefficients take the standard forms:⁵¹

$$C_L(\alpha) = L_1 \alpha \quad (8)$$

$$C_D(\alpha) = D_0 + D_2 \alpha^2 \quad (9)$$

where L_1 , D_0 , and D_2 are constants. [Equation 8](#) assumes lift is zero at $\alpha=0$, which can always be achieved by choice of the origin of α . [Equation 9](#) includes the zero-lift drag D_0 and the induced drag created by the presence of lift.⁵²

Powered flight begins at $\alpha=\alpha_0$, where $C_L(\alpha_0) = L_1 \alpha_0$ is the value of the lift coefficient required to keep the vehicle aloft as powered flight begins. Changing the assumed value of α_0 will change the values of L_1 and D_2 in [Equations 8](#) and [9](#), but will not change the results below, which depend only on D_0 and D_2/L_1^2 , neither of which scale with the assumed α_0 . As a result, our results below do not depend on the choice of α_0 .

For specificity, we assume $\alpha_0 = 2$ degrees. Since we found above that $C_L A = 0.061 \text{ m}^2$ at the start of powered phase, then $L_1 A = 0.0305 \text{ m}^2/\text{deg}$.

We next estimate $D_0 A$ and $D_2 A$ by using information about powered flight and glide phase.

Using [Equation 7](#), the net force accelerating the vehicle is:

$$T_{net} = T - F_{drag} = T - C_D A q_0 \quad (10)$$

where T is the thrust generated by the engine.

We use [Equations 8](#) and [9](#) to express the drag coefficient in terms of the lift coefficient, which allows us to estimate the drag coefficient during powered flight by relating it to the lift needed to keep the vehicle at constant altitude as the propellant mass decreases:

$$C_D = D_0 + D_2 \left(\frac{C_L}{L_1} \right)^2 \quad (11)$$

Equation 10 then becomes:

$$T_{net} = T - q_0 D_0 A - q_0 D_2 A \left(\frac{Mg\lambda}{q_0 L_1 A} \right)^2 \quad (12)$$

where Equation 5 has been used relate the lift coefficient to vehicle mass, which is a function of time:

$$M(t) = M(0) - \dot{m}_f t \quad (13)$$

The increase ΔV in speed during powered flight is given by:

$$\Delta V = \int_0^{t_b} \frac{T_{net}}{M(t)} dt \quad (14)$$

where t_b is the burntime.

The thrust and the specific impulse, I_{sp} , of a scramjet engine are related by:⁵³

$$T = \dot{m}_f g I_{sp} \quad (15)$$

As noted above, the thrust, and therefore I_{sp} , is roughly proportional to $1/V$, which is seen in plots of I_{sp} against Mach number.⁵⁴ For our calculations, we assume that at Mach 5 the thrust is 4,450 N (1,000 lbf), which is the upper end of the range given for the thrust produced by the Pratt & Whitney SJY61 scramjet engine that powers the X-51A.⁵⁵ Assuming $\dot{m}_f = 0.57 \text{ kg/s}$ (based on the reported fuel burn rate during the test flight), Equation 15 shows that this corresponds to a specific impulse of about $I_{sp} = 800 \text{ s}$, which is consistent with data released by the U.S. Air Force.⁵⁶ For our calculations, during flight we scale I_{sp} with one over the vehicle's velocity relative to this value of I_{sp} at Mach 5.

To calculate ΔV we insert Equations 12 and 13 into Equation 14, assume $I_{sp} = 800 \text{ s}$ at Mach 5 and $\dot{m}_f = 0.57 \text{ kg/s}$, and use an average value $q_0 = 107.5 \text{ kPa}$ during powered flight. We then numerically integrate Equation 14, varying the constants D_0 and D_2 to give (1) the value of ΔV reported

from the 2013 X-51A flight test (80 m/s), and (2) the maximum value of L/D consistent with the reported glide during descent in the 2013 test, which we consider next.

Descent phase and L/D

Following the end of powered phase the vehicle glides to splash down in the ocean. The range and time of the glide can give an estimate of its maximum value of L/D . To better understand the aerodynamics of the vehicle, during descent the operators conducted various maneuvers of the vehicle, which affected its glide distance.

As discussed, during powered flight the vehicle was flown at angles-of-attack below those that maximize L/D , but once powered phase ends it would make sense to increase α to maximize L/D to maximize the glide range. This appears to have been done during flight tests of the X-43A.⁵⁷ In the X-51A case, we find that this change in α increases the flight altitude of the vehicle from about 19.4 km at the end of powered flight to 24.2 km as it begins glide phase. This ending value is found from Equation 6 using $\alpha = 1.6$ degrees at the end of powered phase and $\alpha \sim 3.5$ degrees for maximum L/D (see below).

That increase in altitude will lead to a small decrease in speed, which can be estimated by calculating the tradeoff of kinetic for potential energy:

$$0 = \Delta E = \Delta \left(\frac{mV^2}{2} + mgh \right) \quad (16)$$

so that:

$$\Delta V = -\frac{g\Delta h}{V} \quad (17)$$

An altitude change of 5 km at a speed of Mach 5 (1,475 m/s) would decrease V by about 33 m/s, or 2%. We ignore this change in the range estimates in the following sections, which therefore slightly overestimate the glide ranges, but include it here in estimating L/D .

A detailed report on the 2013 X-51A test flight states that during descent “aerodynamic parameter identification (PID) maneuvers were to be performed at Mach numbers 5, 4, 3, and 2. After almost 5 minutes of descent, the X-51A splashed down in the Pacific Ocean, approximately 340 nm [630 km] downrange.”⁵⁸

We use numerical computations to estimate what value of L/D would give this combination of glide time and range. We assume that the vehicle maximizes L/D during glide and that the PID maneuvers do not

significantly reduce the glide range.⁵⁹ We also assume that the vehicle maintains a bearing directly down-range throughout glide. These assumptions may underestimate somewhat the vehicle's actual maximum value of L/D; in the analysis below we consider the effect of increasing the value of L/D.

Our glide analysis gives a maximum value of L/D of about 1.8.⁶⁰ In particular, assuming L/D = 1.8 and that glide started at a speed of 1,472 m/s (Mach 5.1 minus the 33 m/s lost upon climbing to a higher altitude at the start of glide) at an altitude of 24.2 km and that the vehicle has a ballistic coefficient $\beta = M/(C_D A) = 9440 \text{ kg/m}^2$,⁶¹ splashdown in the ocean would occur after a glide of 337 s (5.6 min) and a distance of 258 km. From reports on the test we estimate that the powered phase ended at a distance of 345 to 355 km from the point at which the booster and vehicle were dropped from the B-52. Assuming "downrange" means relative to that drop point, then the total downrange distance would be about 610 km. The fact that maneuvers were conducted during descent would change the time and distance somewhat compared to a simple glide, such that this estimation of L/D should be considered an approximation.⁶²

For the rest of our analysis, we assume the base case has a value of L/D = 1.8 as the vehicle glides during its descent, but we consider how higher values of L/D would change the total range of the vehicle.

We now have approximate values from the X-51A final test for the velocity change during powered flight ($\Delta V = \text{Mach } 5.1 - \text{Mach } 4.83 = 1,505 - 1,425 \text{ m/s} = 80 \text{ m/s}$), the maximum value of L/D (1.8), and the curve of lift versus α (with $L_1 A = 0.0305$). Using [Equation 14](#) with the parameter values discussed above, we fit $D_0 A$ and $D_2 A$ to give values that give this velocity increase during powered flight and maximum value of L/D. This process gives $D_0 A = 0.03245$ and $D_2 A = 0.00220$. The resulting curves for lift, drag, and L/D are shown in [Figure 3](#). During the powered phase, α changes between 1.6 and 2 degrees (which correspond to the values 0.061 and 0.048 for $C_L A$ found above at the start and end of powered phase), and the estimated L/D varies from 1.3 to 1.5. The maximum value of L/D = 1.8 occurs at about $\alpha = 3.8$ degrees.

Our approximate model of the X-51A therefore assumes the following parameters:

Initial vehicle mass = 677 kg

Final vehicle mass = 557 kg

Mass of interstage + ethylene = 79 kg

Initial mass with booster = 1,790 kg

JP-7 fuel mass = 120 kg

JP-7 burntime = 210 s

JP-7 fuel flow rate = 0.57 kg/s

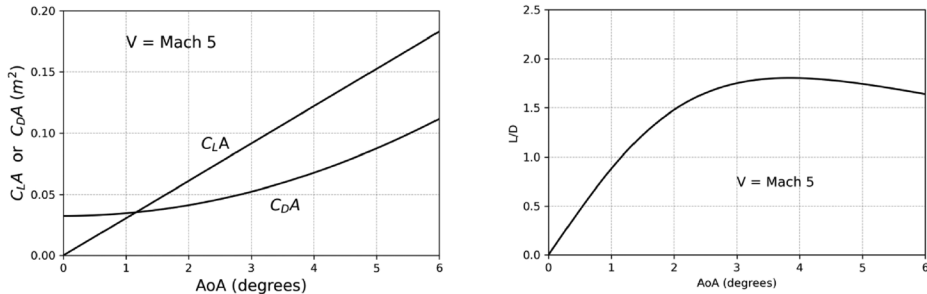


Figure 3. Curves for the lift and drag coefficients (left) and lift-to-drag ratio (right) as functions of angle-of-attack (AoA), for values $L_A = 0.0305 \text{ m}^2/\text{deg}$, $D_A = 0.03245$, and $D_2 A = 0.00220$. During powered flight, $\alpha = 1.6$ to 2.0 degrees. Maximum $L/D = 1.8$ occurs around $\alpha = 3.8$ degrees.

q_0 during powered phase = 107.5 kPa

Thrust at Mach 5 = 4,450 N = 1,000 lbf

I_{sp} at Mach 5 = 800 s

L/D during glide = 1.8

$C_L A$ and $C_D A$ as functions of α given in Figure 3.

Modeling HCMs using variations of the X-51A model

To explore potential capabilities of systems like HAWC and HACM that are based on the X-51A vehicle, we modify the model developed above in several ways.

First, we reflect possible improvements in the engine by increasing the I_{sp} of the scramjet. For the X-51A, we assumed the thrust at Mach 5 was 4,450 N (1,000 lbf), the upper limit reported for its engine, which corresponds to $I_{sp} = 800$ s for $\dot{m}_f = 0.57 \text{ kg/s}$. For the variations below we show the effects of increasing I_{sp} to 900 and 1,000 s. For simplicity, we assume any modifications of the vehicle to increase I_{sp} do not increase the vehicle's mass.

Second, we increase the amount of fuel the vehicle carries. We compare two ways of using this additional fuel: (1) increasing the duration of the powered phase (t_b) with the same fuel flow rate and thrust as the X-51A, and (2) increasing the fuel flow rate to the engine, which will increase the thrust produced for a given value of I_{sp} since $T = g I_{sp} \dot{m}_f$.

In addition to increasing the vehicle mass when adding fuel, we assume the size of the body must be increased since the volume of the X-51A is not large enough to accommodate a significantly greater volume of fuel.⁶³ We assume that the vehicle is scaled up enough to hold the volume of the additional fuel, but retains the same body shape. This will leave the lift and drag coefficients C_L and C_D unchanged but will increase the reference area A . We discuss this scaling in detail below.

Third, we consider the effect of using a more capable booster to accelerate the vehicle to higher initial speed. This was done in the X-43A flight tests, with the booster accelerating the vehicle to speeds near either Mach 7 or Mach 10. This approach is complicated by the fact that scramjet thrust decreases with speed as $1/V$ so for high speeds it may not be able to provide high enough thrust to maintain constant speed.

In addition, [Equation 2](#) shows that at a constant value of dynamic pressure, the airflow to the engine also decreases as $1/V$ (since increasing V will require flying at lower ρ) so the vehicle must be designed to collect a sufficient volume of air at these speeds to be able to oxidize the fuel. This means that the vehicle must be designed to have a large enough air inlet capture area A_{in} for the intended speeds.

Finally, we consider the effect of designing a vehicle with a higher maximum value of L/D , which will increase its glide range at a given speed.

Range calculation

To compare the ranges of HCMs with varying characteristics, we calculate the “hypersonic range” of the vehicle—that is, the range from booster burnout to the point at which its speed falls below Mach 5, which is the definition of hypersonic.⁶⁴

The range of a powered vehicle is commonly expressed by the Breguet equation:

$$R = \frac{L}{D} \frac{VI_{sp}}{\lambda} \ln\left(\frac{M_0}{M_F}\right) \quad (18)$$

which is often written without the inertial factor λ , and where M_0 and M_F are the initial and final masses of the vehicle. However, this equation assumes that the vehicle is traveling at a constant speed and L/D , so it is not generally applicable.⁶⁵ We instead calculate the range in the following way.

If the vehicle speed is V_0 at the start of the powered phase when the scramjet is operating, then following the discussion leading to [Equation 14](#) the speed at time t during powered flight is:

$$V(t) = V_0 + \int_0^t \frac{T_{net}}{M(t')} dt' \quad (19)$$

and the pathlength the vehicle travels during the powered phase is:

$$R_{powered} = V_0 t_b + \int_0^{t_b} \int_0^{t'} \frac{T_{net}}{M(t'')} dt'' dt' \quad (20)$$

where t_b is the burntime. We calculate the speed and range by numerically integrating these equations.

For the speeds considered here, the unpowered glide range of the vehicle starting at V_g and gliding until it slows to V_f can be accurately estimated by $R_{glide} = (L/D)(V_g^2 - V_f^2)/(2g\lambda_g)$, where $\lambda_g = \lambda(V_g)$ is given by Equation 4.⁶⁶ The total range after booster burnout can then be estimated as:

$$R_{tot} = R_{powered} + \frac{L}{D} \frac{V_g^2 - V_f^2}{2g\lambda_g} \quad (21)$$

Under these same assumptions, the time duration of glide is accurately given by $t_{glide} = (L/D)(V_g - V_f)/(g\lambda_g)$, so the total hypersonic flight time is:⁶⁷

$$t_{tot} = t_{powered} + t_{glide} = t_b + \frac{L}{D} \frac{V_g - V_f}{g\lambda_g} \quad (22)$$

To calculate the hypersonic range, we take $V_f = \text{Mach } 5$. We use these equations to calculate the range and time of flight in the analysis below.

Mass calculation

As discussed above, the total mass of the HCM vehicle plus booster is an important parameter, particularly for air-launched weapons. The total mass depends on the mass of the payload the booster must accelerate (which consists of the vehicle, its fuel, and the interstage connecting the vehicle to the booster), the speed to which the booster must accelerate the payload, and details about the booster itself.

To estimate the size of the required booster, we use an approximate equation derived from the rocket equation that assumes the booster has n stages and increases the speed of the vehicle by ΔV . Each stage has a fuel fraction φ (equal to the propellant mass of the stage divided by the total stage mass) and an exhaust velocity V_{ex} , and the total delta-V is equally divided among the stages.⁶⁸

$$\frac{M_{tot}}{P} = \left\{ 1 - \left[1 - \exp \left(-\frac{\Delta V}{nV_{ex}} \right) \right] / \varphi \right\}^{-n} \quad (23)$$

M_{tot} is the total mass of the booster plus payload P . Here P is the mass of the HCM vehicle and the fuel it carries plus the interstage connecting it to the booster.⁶⁹

The total mass of the booster, interstage, and fueled X-51A vehicle was reported to be 1,790 kg. We use this mass and [Equation 23](#) to estimate the parameters of the modified, single-stage ATACM booster used in the tests. In particular, for $n=1$ we find that a booster with $V_{ex} = 2.6$ km/s and $\varphi=0.74$ can accelerate the payload to Mach 4.9 (1,446 m/s), as was reported in the 2013 flight test. In later sections of the paper, we assume $\varphi=0.8$, which is an 8% increase in fuel fraction over 0.74.

Variations of an X-51A-like vehicle

Baseline case: X-51A model with improvements

In the 2013 X-51A test, the powered phase started at a speed of $V_0 =$ Mach 4.83 (1,425 m/s) and increased to Mach 5.1 (1,505 m/s) while burning 120 kg of JP-7 fuel in 210 s ($\dot{m}_f = 0.57$ kg/s), with $I_{sp} = 800$ s. These numbers imply that the vehicle traveled a little over 300 km during this time. While it subsequently glided for several hundred kilometers until it splashed down, it could have maintained velocity above Mach 5 during glide for only about 10 km.

The results of the calculations described above, using the approximate model of the X-51A, are shown in the top row of [Table 1](#). V_g is the speed at the end of powered phase, which we use as the speed at the start of glide, ignoring the small reduction due to the vehicle increasing its altitude at the start of glide.

The lower rows in [Table 1](#) show the results assuming $I_{sp} = 900$ s and 1,000 s at Mach 5. The total increase in range scales roughly with the increase in specific impulse; much of that increase results from the longer glide range due to the higher speed at the end of the powered phase. The total range and time from [Table 1](#) for the case of $I_{sp} = 900$ s, which is higher than that of the X-51A, are shown as the solid gray dot in [Figure 4](#). For comparisons to other variations, we consider this our “baseline case.”

For the following examples, we consider modifications of the base case that have a total mass of 2,300 kg, since that appears to be the mass limit

Table 1. Results for the X-51A model with variations of specific impulse.

I_{sp} (s)	Thrust (N)	V_g (Mach)	$R_{powered}$ (km)	R_{glide} (km)	R_{tot} (km)	t_{tot} (min)	M_{tot} (kg)
800	4,450	5.13	309	11	320	3.6	1,790
900	5,006	5.53	321	47	368	4.0	1,790
1,000	5,563	5.91	333	83	416	4.4	1,790

Results for the case $t_b = 210$ s, $\dot{m}_f = 0.57$ kg/s, $V_0 =$ Mach 4.83. V_g is the speed at the end of powered phase and the start of glide phase; the glide phase ends when the vehicle reaches Mach 5. The value of I_{sp} is the value at Mach 5 and is proportional to $1/V$. The vehicle is assumed to fly at constant $q_0 = 107.5$ kPa. M_{tot} is the estimated mass of the booster plus interstage plus fueled vehicle when boost begins.

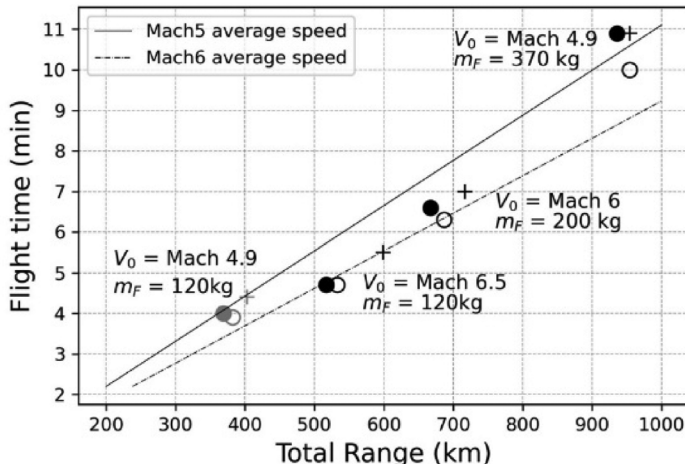


Figure 4. Ranges of variations of the X-51A model versus flight time. All the data points shown assume $I_{sp} = 900\text{s}$. The solid dots assume a fuel mass flow rate of 0.57kg/s while the open circles assume 0.68kg/s . V_0 is the speed to which the vehicle is boosted, and m_F is the mass of JP-7 fuel the vehicle carries. The dots and circles both assume $L/D=1.8$ during glide, while the + markers assume $L/D=3.0$ for a mass flow rate of 0.57 . We consider the solid gray dot as the base case, which is our model for the X-51A but with a higher I_{sp} . The total mass for the booster plus vehicle of the gray points is $1,790\text{kg}$. All the black data points assume a total mass of $2,300\text{kg}$. The solid and dashed lines show average speeds of Mach 5 and Mach 6, respectively. These calculations include only powered and glide phase; adding a ballistic phase is considered below.

for delivering an HCM from fighter aircraft. In calculating the total mass, we use [Equation 23](#) assuming a single stage booster but with a higher fuel fraction ($\varphi = 0.80$) than we estimated for the ATACM booster. We assume that in all cases the vehicle flies at the same value of dynamic pressure as in the X-51A flight tests, which appears to depend on the level of stress and heating the vehicle is designed to withstand. While some of the variations we consider have top speeds higher than that reported for the X-51A tests, reports of the tests said the vehicle was expected to reach speeds greater than Mach 6, so we assume the vehicle could withstand the additional heating of these higher speeds with minimal changes.

Decreasing the burn time to increase the fuel flow rate

The scramjet thrust can be increased by increasing the flow rate of air and fuel to the engine. If the fuel mass is unchanged, this reduces the burn time but keeps the overall vehicle mass the same, so that a booster of the same mass could accelerate the vehicle to the same initial speed (Mach 4.9). We consider a case in which the air and fuel flows are increased by 20% over the baseline case (from $\dot{m}_f = 0.57$ to 0.68kg/s), which results in the gray open circle in [Figure 4](#) for the case of $I_{sp} = 900\text{s}$. This shows that such a change will increase the range by just a few percent. The shorter burn time

of the scramjet gives a shorter range during powered flight when the scramjet is operating, but the higher speed of the vehicle when the scramjet stops burning gives a somewhat longer glide range.

Increasing the fuel flow rate increases the thrust from the scramjet. For $\dot{m}_f = 0.68 \text{ kg/s}$, the thrust is:

$$I_{sp} = 800 \text{ s} : T = 5,330 \text{ N} = 1,200 \text{ lbf}$$

$$I_{sp} = 900 \text{ s} : T = 6,000 \text{ N} = 1,350 \text{ lbf}$$

$$I_{sp} = 1,000 \text{ s} : T = 6,660 \text{ N} = 1,500 \text{ lbf}$$

Boosting to higher initial speed

Both range and average speed can be increased without modifying the vehicle by using a more powerful booster to accelerate the vehicle to a higher initial speed. For Figure 4, we assume a vehicle with the mass of the fueled X-51A (677 kg) (plus interstage) and find that keeping the total mass of booster plus vehicle to about 2,300 kg limits the highest initial speed that can be achieved to a little over Mach 6.5 (1,940 m/s).⁷⁰

Figure 4 shows the resulting range and flight time, the black dots near a total range of 500–550 km, for the case of $I_{sp} = 900 \text{ s}$ and (1) the original 210 s burn time (solid dot) and (2) a shorter burn time that gives a 20% increase in the fuel flow rate, as above (open circle). This leads to roughly a 40% increase in range over the base case (gray dots).

Increasing burn time by burning additional fuel at the original fuel flow rate

For this case we assume that, as in the base case, the booster accelerates the vehicle to Mach 4.9 and the vehicle begins powered flight at Mach 4.83. The vehicle is assumed to burn fuel at the same rate as in the base case. However, we increase the amount of fuel the vehicle is carrying to the maximum amount it can carry while still keeping the total mass of booster plus vehicle to 2,300 kg. This requires increasing the fuel mass from 120 kg to about 370 kg and the burn time from 3.5 minutes (210 s) to just under 11 minutes (650 s).

We assume that carrying this extra fuel will require a larger vehicle. We scale up the X-51A in the following way. We first estimate the volume of the X-51A, which we assume is a cylinder of diameter 0.58 m and length 4.0 m (shorter than the actual 4.3 m length of the X-51A to account for the tapering at the front of the vehicle), giving a volume of 1.06 m³.

We assume that the mass and volume of components within the vehicle remain the same and that the vehicle size is scaled up so that its volume increases by the volume of the additional fuel. We also assume that a quarter of the original 557 kg unfueled mass of the vehicle, or 130 kg, consists of structure and heat shielding that scale with the surface area of the vehicle. This value is used to estimate how the structural mass of

the vehicle scales and its exact value will have little effect on the results below.

The additional mass of JP-7 fuel, $\delta m_{JP7} = 250\text{kg}$, will require an additional volume of about $\delta vol = \delta m_{JP7} / \rho_{JP7}$, where the density ρ_{JP7} of JP-7 fuel is about 800 kg/m^3 , giving an extra volume of $\delta vol = 0.31\text{ m}^3$. We therefore scale the vehicle by a factor of $[(1.06 + 0.31)/1.06]^{1/3} = 1.09$ while keeping the same shape, so that C_L and C_D stay the same. The surface area will increase by a factor of $(1.09)^2 = 1.19$. We assume this larger surface area will add $0.19 \times 130\text{ kg} = 25\text{ kg}$ of structural mass. This scaling increases the reference area A by 19%, which will increase the lift and drag of the vehicle.

The fueled vehicle will therefore have a mass of 952 kg, which results in a total mass of 2,300 kg using a booster that accelerates the vehicle to a speed of Mach 4.9.

Calculating the range and flight time of this larger vehicle, assuming $I_{sp} = 900\text{s}$, gives the solid black dot in the upper right corner of [Figure 4](#).

As above, we also calculate the range and flight time assuming a 20% increase in fuel flow rate while decreasing the burntime by 20% to 520 s. The result of this calculation is shown by the open black circle in the upper right corner of [Figure 4](#). This change leaves the range about the same but reduces the flight time by about a minute.

Boosting to higher speed and increasing the fuel mass

The next variation is intermediate to the previous two. The booster accelerates the vehicle to an initial speed of Mach 6 (1,777 m/s) and carries 80 kg of extra fuel. Using the vehicle scaling described above, this is the maximum amount of fuel that can be added for this initial speed while keeping the total mass at 2,300 kg. At the X-51A fuel flow rate of $\dot{m}_f = 0.57$, this fuel mass gives a burntime of 350 s (we note that HAWC's scramjet was reported to have burned for 327 s in one of its flight tests⁷¹).

Scaling up the vehicle to carry the extra fuel, as above, requires a scaling factor of 1.03, so that the surface area increases by a factor of 1.06. This adds about 8 kg of structural mass, so the total fueled vehicle mass is 765 kg.

The result is shown as the solid black dot near the center of [Figure 4](#), not surprisingly with range and flight time intermediate to the previous two cases. As above, the open black circle shows the results assuming a roughly 20% increase in fuel flow rate and 20% decrease in burntime to 300 s.

Increasing L/D

The final variation we consider is increasing the maximum value of L/D, which will primarily enhance the vehicle's flight during its glide phase. We consider a two-thirds increase in the maximum L/D from our estimate of 1.8 for the X-51A to a value of 3.0. We note that in its flight tests the X-43A

vehicle appeared to show a maximum L/D in the range of 2.6 to 2.8;⁷² because it had a larger lifting area than the X-51A relative to the size of the vehicles, one would expect it to have a higher L/D value than an X-51A-like vehicle. We also note that the Common Hypersonic Glide Body (C-HGB) currently being developed by the Army and Navy appears to have L/D around 2.2.⁷³

For this variation we recalculate the drag coefficients D_0 and D_2 in [Equation 9](#) as described above to give a drag coefficient as a function of α that leads to a maximum L/D of 3.0. This leads to $D_0A = 0.0368 \text{ m}^2$ and $D_2A = 0.0007$, which are used to calculate the new range.

For each of the above variations, [Figure 4](#) shows the effect of this increase of L/D on the cases represented by the solid dots and is shown by the grey and black plus signs. The increase in L/D leads to only a small change in range during the powered phase and about a two-thirds increase in the glide range, which corresponds to a much smaller percentage increase in total range since the glide range is significantly shorter than the powered range. Recall we are calculating the hypersonic range of the vehicle, which is its range while traveling above Mach 5. Since the speed at the end of powered flight, which is the start of the glide phase, is not much above Mach 5 in many of these cases, the glide range is relatively short, so this change does not make a substantial difference. The difference is greatest in the case in which the vehicle was boosted to Mach 6.5, since this case has the largest speed at the start of glide phase.

Discussion

These examples lead to the following conclusions.

As a baseline, we have modeled a vehicle similar to the X-51A that was test flown in 2013 and assume the vehicle can be scaled up to carry additional fuel. We also assume this vehicle is designed to be launched from U.S. fighter aircraft and in our variations have therefore restricted the total mass of booster plus vehicle to 2,300 kg.

The black symbols in [Figure 4](#) show the capabilities of vehicles with a total mass of 2,300 kg. As discussed, the vehicle mass increases when it is carrying additional fuel, and the booster mass increases if it must launch a more massive vehicle or accelerate a vehicle to a higher initial speed. [Figure 4](#) therefore shows the different ways in which 2,300 kg of booster plus vehicle mass can be configured, and the tradeoffs between range and delivery time that result from the limit on total mass.

[Figure 4](#) shows that the total hypersonic range of these vehicles is limited by their relatively low speed, which is restricted by the fact that the scramjets burn hydrocarbon fuel. These vehicles have average speeds of roughly Mach 6 or below.

The low speed of these vehicles also means they would likely be vulnerable to interception by terminal missile defenses. Attempting to boost

them to higher speed does not solve this problem since the scramjets themselves will not work above about Mach 7, while our previous study showed that evading defenses requires a speed of Mach 9–10 as the vehicle starts its dive to the target.⁷⁴

Figure 4 also shows that, with the constraint that the total mass = 2,300 kg, the main determinant of total range for a vehicle of this type is the amount of fuel it carries: Total range appears to scale roughly with the square root of the fuel mass. To maximize the range under this constraint, the vehicle should be launched at a low speed to reduce the mass of the rocket booster and allow the vehicle to carry additional fuel.

Table 1 shows that increasing the specific impulse is a relatively effective way to increase capabilities: Increases of 11–12%, from 800 s to 900 s, or 900 s to 1,000 s, lead to increases of missile range by 10–15%. How difficult achieving such increases in I_{sp} might be is unclear.

Increasing the fuel flow rate by 20% for the same total fuel mass, which increases the thrust but decreases the burn time, increases the range by only a couple percent, but at the longest ranges can decrease the flight time by 5–10%. Increasing the maximum L/D by 67% has little effect except at the highest speeds considered here, where it increases the range by about 15%.

Figure 4 shows that the U.S. Air Force goals mentioned above from 2013, that an X-51A-like vehicle could fly a range of 900 to 1,100 km with a delivery time of 10 to 12 minutes, appear compatible with modifications that could be made to the baseline X-51A vehicle, and our analysis shows what improvements over the X-51A are required to reach these ranges.

The specific improvements over the X-51A test vehicle assumed in Figure 4 are:

- I_{sp} can be increased from 800 s to 900 s,
- The amount of fuel the vehicle can carry can be increased by scaling up the vehicle but with no other major changes,
- Air and fuel flow rates to the combustor can be increased by 20%,
- The fuel fraction of the booster can be increased by 0.74 to 0.80.

Further increasing the capabilities of such a vehicle would require additional improvements and likely require weapons with greater total mass, which would therefore be less compatible with air-launching (although they could be carried by large aircraft like a Boeing B-52 strategic bomber). In any case, the capability of these vehicles would still be limited by the fact that their top speeds would be less than about Mach 7.

The variations shown in black in Figure 4 will have higher speeds and longer flight times than the baseline case shown in gray. Assuming q_0 is the same in all cases, then the level of stress on the vehicle, which scales with q_0 , should also be essentially the same. We noted that the X-51A

was reportedly designed to reach speeds above Mach 6, so it should also be able to withstand the heating rates, which scale roughly as $\rho V^3 \sim q_0 V$, in the variations we consider. However, the duration of heating (“heat soak”) will be 2 to almost 3 times longer than the baseline for several of these variations, which might require additional insulation.

We also assume that the air inlet capture area A_{in} (Equation 2) is large enough that the air flow to the engine at these higher speeds and altitudes is not a limitation.

Comparison of HCMs to BGVs and MaRVs

Maneuvering of HCMs and BGVs

HCMs, BGVs, and MaRVs are all designed to maneuver during the final phase of their flight as they dive to the ground. This terminal maneuvering can be used to increase their accuracy, to attempt to evade missile defenses, and even to retarget by hundreds of kilometers.

HCMs and BGVs can also maneuver during the midcourse phase of their flight since, unlike MaRVs, they fly at low altitudes for significant portions of their trajectories and can use atmospheric forces to create forces for turning.

Midcourse maneuvering is often given as a key rationale for developing hypersonic weapons.⁷⁵ Such maneuvering is presented as allowing them to follow complicated paths to fly around areas containing radars or defenses, to carry out surveillance over regions of interest, or to retarget over very large areas. However, the amount of possible maneuvering for these vehicles is typically overstated: Because of their very large speed, hypersonic weapons require large forces to turn, which limits the amount they can turn and can make such turns slow and costly.

In a previous paper, we analyzed the maneuvering of BGVs.⁷⁶ Here we compare maneuvering of a BGV to maneuvering by an X-51A-like HCM.

BGV maneuvering. A BGV flying at an angle of attack that maximizes its L/D can maneuver by diving to regions of higher atmospheric density to increase its total lift $C_L A q_0$, while banking to divert part of the total lift to generate a lateral force. By dropping to a lower altitude without changing its speed, the vehicle increases q_0 , and therefore the lift force, by the ratio of the atmospheric densities at the two altitudes.⁷⁷ Larger changes in altitude lead to higher forces and shorter times required to make a given maneuver. However, they also lead to large increases in both the stress and heating of the vehicle since those are proportional to q_0 , which depends on altitude. Limits on the amount of stress and heating the vehicle can withstand will limit how much and how fast it can maneuver.

Dropping to lower altitudes and increasing q_0 will also increase the drag on the vehicle, which will slow it and reduce its glide range. Conducting larger or faster maneuvers will lead to greater reductions in range.

Figure 5 below shows the range losses associated with maneuvering for a BGV with a maximum range of about 660 km, which is boosted to Mach 9.4 (2,760 m/s), has an average speed of about Mach 7, and has $L/D = 2.2$. These calculations are described elsewhere.⁷⁸ To complete a turn in three minutes, which is more than half of its total flight time, it would need to drop from its initial altitude of 35 km by about 1.5 km to turn by 30° and by 3.5 km to turn by 60° . These drops would increase q_0 , and therefore the stress and heating, by 25% and 67%, respectively, which may not be possible for the vehicle to withstand.

This increase in q_0 would also increase the drag force by 25% and 67% for the 30° and 60° turns, respectively. The extra drag would reduce the distance the vehicle could travel compared to the non-maneuvering case by about 15% and 40%, respectively. These results are shown by the gray curves in Figure 5.

HCM maneuvering. A vehicle like the X-51A can maneuver in a different way. As discussed above, because q_0 is large, the vehicle flies at a small angle-of-attack α during powered flight—less than the value that maximizes L/D . Increasing α by a small amount can increase C_L at constant q_0 to add

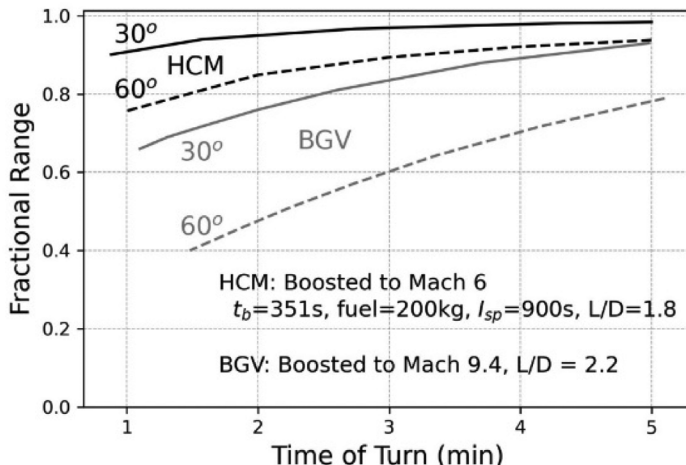


Figure 5. Range reductions as a function of amount and rate of maneuvering. These curves show the fractional range of vehicles, which is the range on a maneuvering trajectory divided by the range with no maneuvering, as a function of the angle of the turn and the time over which the turn takes place. The gray curves are for a BGV and the black curves are for an HCM, with details given in the plot. In both cases, for no maneuvers the hypersonic ranges are about 660 km, and the flight times are 5.1 minutes for the BGV and 6.6 minutes for the HCM.

lift that can be used for maneuvering with a relatively small increase in drag.

To see this, assume the vehicle is traveling with speed V_0 , angle-of-attack α_0 and constant dynamic pressure q_0 . The initial lift is:

$$F_L^0 = C_L^0 A q_0 = Mg \lambda_0 \quad (24)$$

Increasing to a larger angle-of-attack α_1 gives $C_L^1 > C_L^0$, leading to a larger lift force:

$$F_L^1 = C_L^1 A q_0 \quad (25)$$

Increasing α will also increase in drag force, which will reduce the vehicle's speed somewhat, to V_1 .

Assume that as α increases the vehicle banks by an angle θ so that the vertical force F_v^1 keeping the vehicle aloft during the maneuver is:

$$F_v^1 = F_L^1 \cos \theta = C_L^1 A q_0 \cos \theta = Mg \lambda_1 \quad (26)$$

Equating Equations 24 and 26 and assuming for this small change in speed that $\lambda_0 = \lambda_1$, gives:

$$\cos \theta = \frac{C_L^0}{C_L^1} \quad (27)$$

For small angles $C_L A = L_0 \alpha$, so Equation 27 becomes:

$$\cos \theta = \frac{\alpha_0}{\alpha_1} \quad (28)$$

where, using Equations 8 and 24:

$$\alpha_0 = \frac{Mg \lambda_0}{L_1 A q_0} \quad (29)$$

The horizontal force that can be used for maneuvering is:

$$F_\perp^1 = F_L^1 \sin \theta = F_v^1 \tan \theta = Mg \lambda_1 \tan \theta \quad (30)$$

Increasing the angle-of-attack to α_1 increases the drag coefficient to C_D^1 ; the drag force becomes:

$$F_D^1 = C_D^1 A q_0 \quad (31)$$

For small angles the drag coefficient has the form:

$$C_D = D_0 + D_2 \alpha^2 = D_0 + D_2 \left(\frac{M(t) g \lambda}{q_0 L_1 A \cos \theta} \right)^2 \quad (32)$$

where D_0 and D_2 are constants, and the last equality uses Equations 28 and 29. This gives:

$$\frac{C_D^1}{C_D^0} = \frac{D_0 + D_2 \alpha_0^2 \sec^2 \theta}{D_0 + D_2 \alpha_0^2} = 1 + \frac{\tan^2 \theta}{1 + \frac{D_0}{D_2 \alpha_0^2}} \quad (33)$$

where the last step uses the identity $1 + \tan^2 \theta = \sec^2 \theta$. Equation 33 also gives the ratio of drag forces.

Equations 31 and 32 give the net force accelerating the vehicle as:

$$T_{net} = T - F_{drag} = T - C_D A q_0 = T - q_0 D_0 A - q_0 D_2 A \left(\frac{M g \lambda}{q_0 L_1 A \cos \theta} \right)^2 \quad (34)$$

where T is the thrust from the engine.

Using this expression for T_{net} , we can calculate the vehicle's velocity and range during the turn by integrating Equations 19 and 20.

The force F_\perp turns the vehicle by creating a lateral horizontal velocity V_\perp . Since F_\perp always acts perpendicular to V it will rotate V but not change its magnitude. The force will rotate the velocity vector by an angle κ , which can be calculated using:

$$d\kappa = \frac{dV_\perp}{V} = \frac{1}{V} \frac{F_\perp}{M} dt = \frac{g \lambda \tan \theta}{V} dt \quad (35)$$

since $dV_\perp = (F_\perp/M) dt$, where κ is in radians and $V(t)$ is given by Equation 19. The angle the vehicle turns in a time t is then:

$$\kappa(t) = \int_0^t \frac{g \lambda \tan \theta}{V(t')} dt' \quad (36)$$

Numerically integrating Equations 19, 20, and 36 gives the time required to turn by an angle κ for different values of θ , and can be used to calculate how much the additional drag during the maneuver reduces the overall pathlength the vehicle can travel. Since the speed at the end of powered phase will be reduced by the additional drag, the glide range

following the powered phase will be shorter than in the non-maneuvering case.

Example for an X-51A-like vehicle. Using the equations above we repeat the maneuvering calculation done above for the BGV for the case of an HCM.

We consider an X-51A-like HCM that, like the BGV above, has a range of about 660 km, including both powered and glide phases. For this example we use the model considered above that assumes a variation of the X-15A model that is boosted to Mach 6 (1,780 m/s), has $I_{sp} = 900$ s and $L/D = 1.8$, and carries 200 kg of fuel burned over 351 s.

The black curves in Figure 5 show the results. In this case, turning by 30° and 60° in three minutes, as in the BGV case, increases the drag by 7% in the first case and about 23% in the second, which is considerably lower than for the BGV.⁷⁹ This drag reduces the total pathlength by 3% and 11%, respectively. Since q_0 and V remain constant during these maneuvers, the stress and heating only increase due to the increase in the drag coefficient, which in these cases is 7% and 23%.

Note that using this method to maneuver a BGV, by increasing its angle-of-attack, is less efficient than the method of changing altitude discussed above. In the latter case the drag increased by a factor of $1/\cos\theta$, where θ is the bank angle. If instead, maneuvering is done by increasing the angle-of-attack, the ratio of drag forces is:

$$\frac{F_D^1}{F_D^0} = \frac{\left(\frac{L}{D}\right)^0}{\left(\frac{L}{D}\right)^1} \frac{1}{\cos\theta} \quad (37)$$

L/D will be maximum at the angle-of-attack of its normal glide trajectory— $(L/D)^0$ —so changing α to increase lift would reduce L/D to $(L/D)^1$ and therefore give a higher drag force.

These comparisons show that an HCM could maneuver with significantly less range penalty than a BGV of the same range. This difference results in large part due to the different speeds of the two vehicles: The BGV speed during the turn is higher than the HCM speed, so that the BGV requires a larger F_\perp to turn. The difference also arises partly from the fact that if α is near the minimum of the drag curve in the HCM case (Figure 3), small changes in α required to increase lift will result in relatively small changes in drag.

This dependence on speed implies that going to even lower speeds would further reduce the costs of maneuvering. As a result, supersonic

cruise missiles would likely be preferable to HCMs for missions that prioritize maneuverability over speed, such as surveillance missions.

Range vs. mass of HCMs, BGVs, and MaRVs

Above we considered modifications of a vehicle based on the X-51A and how those modifications would affect its mass and capabilities. Since a key interest in HCMs is developing hypersonic weapons with low total mass M_{tot} of booster plus vehicle, in this section we compare the range of HCMs, BGVs, and MaRVs as a function of M_{tot} .

We showed above that a vehicle similar to the baseline X-51A would have a hypersonic range of less than 400 km, but the range could be increased by adding fuel and by boosting it to higher initial speeds than in its flight tests (Figure 4). Below we assume that the vehicle's fuel can be increased by about 300 kg from 120 kg, which was the amount in the X-51A, to 420 kg, which increases the burn time t_b from 3.5 minutes (210 s) to more than 12 minutes (735 s), using a fuel flow rate of 0.57 kg/s. We assume that a different vehicle would be needed for even larger loadings. As above, we consider cases in which the booster accelerates the HCM vehicle to speeds V_H = Mach 5, Mach 6, and Mach 6.5 at the beginning of powered phase. We assume here that $I_{sp} = 900$ s at Mach 5, and maximum $L/D = 1.8$.

M_{tot} for an HCM is determined by the speed V_H to which the booster accelerates the vehicle, and the total payload mass the booster is carrying, as shown in Equation 23. The payload includes the mass of the HCM vehicle and its fuel, the additional structural mass due to scaling up the vehicle to contain the additional fuel, and the mass of the interstage that attaches the vehicle to the booster. We described above how the additional structural mass is calculated and assume the interstage mass is 10% of the vehicle plus fuel mass, which gives a mass similar to the reported interstage mass for the X-51A.⁸⁰

The calculation of M_{tot} shows an important tradeoff in comparing these systems. HCMs can increase their range by burning fuel to create thrust, but at the cost of carrying fuel that increases their mass. Since BGVs and MaRVs do not carry fuel, the payload accelerated by the booster will be lighter than for the HCM case, and the difference in payload mass can be used to make a larger booster while keeping the total mass the same as for the HCM. Both the smaller payload and larger booster will increase the speeds to which the booster can accelerate the BGV and MaRV (V_B and V_M) compared to the HCM for the same M_{tot} .

The difference in booster burnout speeds is illustrated in Figure 6 for the case in which the HCM is boosted to Mach 5 (1,475 m/s) and carries a fuel mass of 120 to 420 kg as discussed above, which changes M_{tot} for

the HCM. Figure 6 shows the speeds that a 500 kg BGV and 400 kg MaRV could have for the same M_{tot} ; the choice of these masses is explained below.

HCM curves. The HCM ranges shown in Figure 4 above include only the powered and glide phases, assuming that the powered phase starts very soon after booster burnout. This was true in flight tests of HCMs, where the scramjet reached full power very shortly after booster burnout. For an HCM, if it is possible to delay the start of the scramjet engine and add a ballistic phase, that process could increase the HCM range.

The ballistic phase would be similar to the first part of the trajectory of a BGV. In both cases the booster gives the vehicle a loft angle γ at booster burnout. The vehicle then follows a ballistic trajectory until it descends into thicker atmosphere where it conducts a pull-up maneuver to put it on a horizontal trajectory at the proper altitude to start its glide phase in the case of a BGV, or its powered phase in the case of an HCM.⁸¹ For BGVs, the ballistic phase typically makes up about half the total range.

If an HCM included a ballistic phase, then the scramjet would not begin producing thrust until after it entered the atmosphere, and the total hypersonic range would include distance traveled during the ballistic, pull-up, powered, and glide phases.⁸² Because the burnout speed of the HCM would be lower than a typical BGV of the same total mass, its ballistic phase would be shorter.

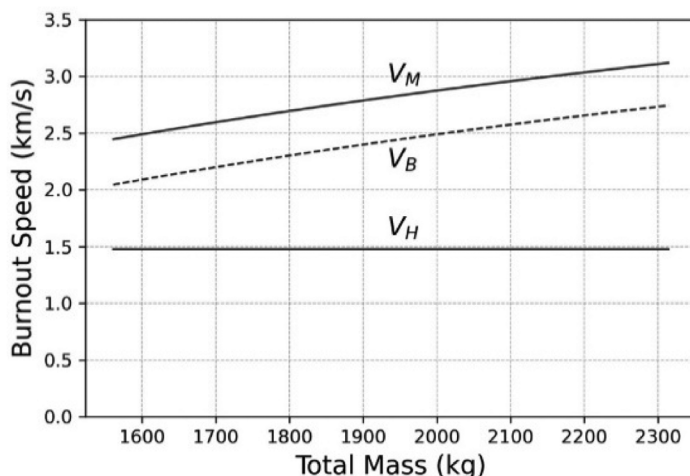


Figure 6. Burnout speeds of BGV and MaRV models compared to an HCM of the same total mass with a constant burnout speed of V_H = Mach 5 (1,475 m/s). Here the HCM is carrying a fuel mass of 120 to 420 kg, which changes its total mass M_{tot} . A 500-kg BGV and 400-kg MaRV with the same M_{tot} could have larger boosters and therefore higher speeds V_B and V_M at booster burnout, which are shown by the upper curves. These calculations assume $n=2$, $V_{ex} = 2.6 \text{ km/s}$, and $\varphi=0.80$ in Equation 23 for the booster mass, and assume the payload includes an interstage that is 10% of the vehicle mass (including fuel in the case of the HCM).

We therefore assume a booster burnout speed V_H and compare two range calculations. In the first case we assume the powered phase starts immediately after booster burnout and at the required altitude, which is determined by V_H and the desired value of q_0 . In the second case, we assume that—as for the BGV—burnout occurs at a loft angle γ , followed by a ballistic phase and a pull-up phase that puts it on level flight at the required altitude, at which point powered phase begins. This process is discussed in detail in our analysis of BGV trajectories.⁸³

Drag during the pull-up maneuver will slow the vehicle, so in this case the powered phase following a ballistic phase will start at a lower speed than it would in the first case for the same burnout speed. Larger loft angles lead to longer ballistic phases but also to greater speed loss during pull-up, which reduces the range of the powered and glide phases but may increase the total range. Larger loft angles also increase the flight time.

[Figures 7–9](#) show in black the HCM range for fuel loadings between 120 and 420 kg, both with a ballistic phase (dashed curve) and without (solid curve). In the cases with a ballistic phase, for each total mass we calculate the range assuming the largest loft angle that still allows the HCM vehicle to reach hypersonic speed during its powered phase (for large loft angles the pull-up maneuver can reduce the speed at the start of powered phase below Mach 5).⁸⁴ We also assume burnout occurs at about 40 km altitude, which is what we assume for the BGV.⁸⁵

These figures also show the ranges of a BGV and MaRV that have the same total mass as the HCM plus booster.

The calculations below were done with a change from those above. The curves in [Figure 4](#) assumed a booster similar to the one used in the X-51A flight tests, which was a modified version of a one-stage ATACM booster, although we assumed a higher fuel fraction than our estimates of the one used in the flight tests.

Using a two-stage booster would be more efficient and give a somewhat smaller booster mass, although because the HCM is accelerated to relatively low speeds, this change would not make a big difference in its total mass. However, using a two-stage booster would be significantly more efficient in the BGV and MaRV cases, since they are accelerated to higher speeds.

We assume that if a military were building a new type of weapon for which speed and mass were a priority, that design would include an optimized booster rather than relying on existing motors, as were used in tests. Booster technology is well-developed, and one would expect that aspect to be a straightforward part of the overall design process. The calculations below therefore assume a two-stage booster for all three systems (HCM, BGV, and MaRV). Aside from that change, the HCM calculations are done in the same way as described above.

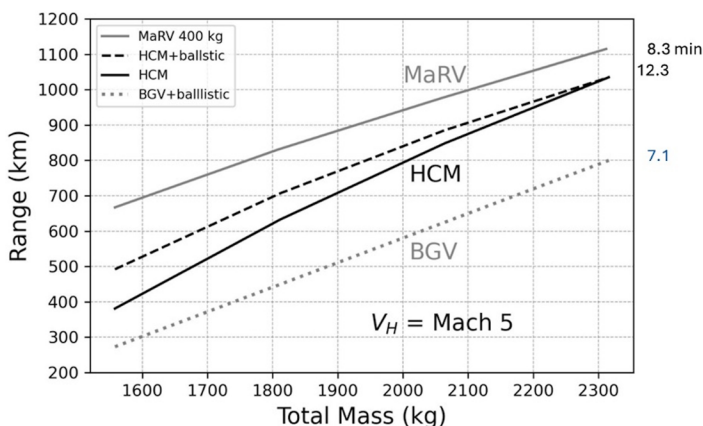


Figure 7. A comparison of range versus total mass for various vehicles, assuming the HCM is boosted to an initial speed of V_H = Mach 5. In these curves, the HCM carries between 120 to 420 kg of fuel, which increases the burn time t_b from 3.5 minutes (210 s) to more than 12 minutes (735 s). The total mass is the mass of the vehicle, fuel, interstage, and extra structural mass from scaling up the vehicle to hold the fuel, plus the booster. The black curves show the HCM range with (dashed) and without (solid) a ballistic phase. The burn-out speeds of the BGV and MaRVs assume vehicle masses of 500 and 400 kg, respectively, and the same total mass as the HCM, and the resulting ranges are shown by the gray dotted curve (BGV) and gray solid curve (MaRV). If the MaRV mass could be made less than 400 kg, which is likely, the gray MaRV curve would move upwards, as shown in Figure 10. The times on the right edge of the plot are the flight time in minutes of the longest-range trajectories shown for each curve.

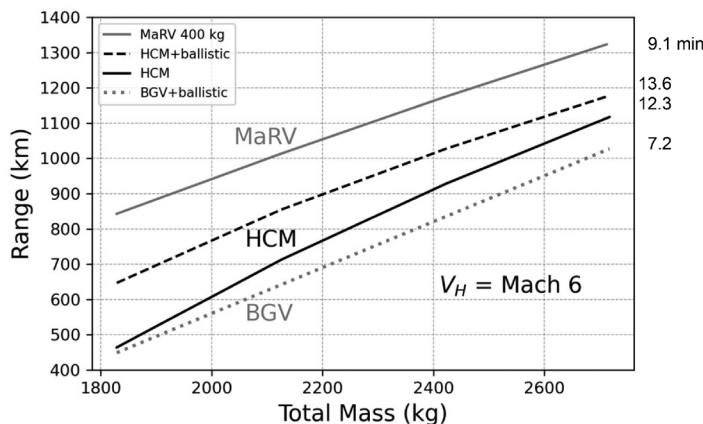


Figure 8. A comparison of range versus total mass for various vehicles, assuming the HCM is boosted to an initial speed of V_H = Mach 6. Other details as in Figure 7.

The calculations below consider HCM models with total masses up to about 3,000 kg. The models at the upper end of this mass range would be too heavy to carry on some aircraft, although the Mayhem vehicle discussed above is reported to be air-launched and may have a mass of about 3,000 kg.⁸⁶ These and heavier vehicles could be launched from other platforms, including

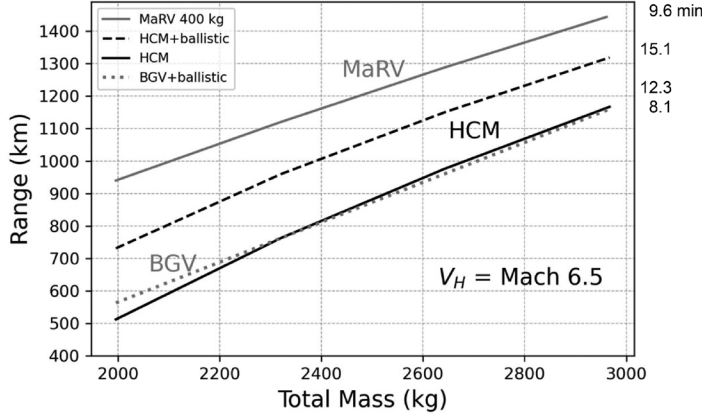


Figure 9. A comparison of range versus total mass for various vehicles, assuming the HCM is boosted to an initial speed of $V_H = \text{Mach } 6.5$. Other details as in Figure 7.

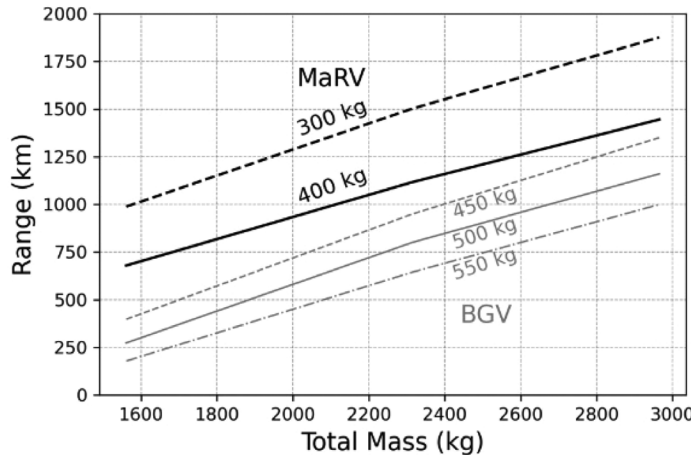


Figure 10. Range versus total mass for different values of the BGV (gray curves) and MaRV (black curves) vehicle masses. These calculations assume $n = 2$, $V_{ex} = 2.6 \text{ km/s}$, and $\varphi = 0.80$ in Equation 23 for the booster mass, and assume the payload includes an interstage that is 10% of the vehicle mass.

ships, like the Russian Zircon. Significantly larger HCMs not designed for air-launching could use different designs for the HCM vehicle.

BGV curves. The BGV hypersonic range is calculated assuming a burnout speed V_B based on M_{tot} as discussed above, and at a loft angle γ chosen to give a hypersonic glide range equal to the sum of the ranges of its ballistic and pull-up phases.⁸⁷ Glide range is calculated until the vehicle slows to Mach 5.

We assume that the BGV has a higher maximum value of L/D than the HCM (2.2 vs. 1.8) since there are fewer constraints on its design than on the HCM vehicle design. Moreover, HCM features like the engine inlet

can increase the drag of the vehicle. $L/D=2.2$ is the value estimated for the BGV currently being developed by the Army and Navy.⁸⁸

The payload for the BGV will be less massive than that of the HCM since it does not include fuel. The BGV vehicle may also have lower mass than the 557 kg of the HCM vehicle (the X-51A mass without fuel) because it does not carry the fuel pumps and other equipment related to operating the scramjet. While the BGV's average speed in the atmosphere will be higher than the HCM, it can be flown at a lower value of q_0 since it can maintain higher altitudes, which helps mitigate stress and heating during glide. However, the HCM has the advantage that it is actively cooled by circulating its fuel to absorb heat from the vehicle surface, which presumably reduces the amount of heat shielding required.

It is therefore not clear whether the BGV vehicle mass can be reduced significantly below that of the empty HCM vehicle. In the comparisons below we assume the BGV can be made 10% lighter than the HCM and has a mass of 500 kg. [Figure 10](#) shows how the range changes with total mass for different values of the BGV vehicle mass between 450 and 550 kg.

The BGV results are shown as the gray dotted curves in [Figures 7–9](#). These figures show that for equal total masses, the 500 kg BGV has a shorter range than the HCM with a ballistic phase for all the cases considered here. This is because of the significantly higher speed required by the BGV to reach the same range as the HCM, which drives up the booster mass more than adding fuel to the HCM.

MaRV curves. [Figures 7–9](#) show that the comparison to MaRVs is quite different. Since MaRVs do not experience the stress and heating of a long glide phase in the atmosphere, they can be made significantly less massive than an HCM or BGV. For example, in the 2000s the United States flight-tested a MaRV being developed for the Conventional Trident Modification (CTM). It was based on the Mk-4 reentry vehicle with flaps for aerodynamic maneuvering that gave high accuracy and was intended to carry a warhead that released a spray of tungsten rods.⁸⁹ The intended range of the CTM was more than 6,000 km and it had a much higher reentry speed (near Mach 20) than the systems considered here, yet the MaRV's mass was reported to be only 250 lb (114 kg).⁹⁰

The calculations for [Figures 7–9](#) conservatively assume a MaRV vehicle mass of 400 kg—more than three times larger than the MaRV tested for the CTM. If the MaRV mass were less than 400 kg, its burnout speed and therefore its range would increase compared to the black curves in [Figures 7–9](#); [Figure 10](#) compares its range to that of a 300-kg MaRV.

The MaRV hypersonic range is calculated on a trajectory that assumes that booster burnout gives a speed V_M based on M_{tot} as discussed above, loft angle 40°, and altitude 40 km. Even though the MaRV requires a

higher speed than the HCM to reach the same range, the smaller MaRV mass keeps M_{tot} smaller than for the HCM for all ranges considered.

Comparison

Figures 7–9 show that for all the cases considered here, the MaRV has a longer range and shorter flight time than the HCM and BGV for the same total mass. This is especially true for systems with low total mass. Moreover, if the MaRV vehicle mass were less than 400 kg, its burnout speed and therefore its range would increase relative to that shown here, for the same M_{tot} .

In addition, calculations for Figure 7 show that for $M_{tot} = 2,300$ kg, the HCM can reach a range of 1,030 km in 12.8 minutes while a MaRV of that mass could reach that range in about 7 minutes—a flight time more than 40% shorter.

The upper end of the range and mass calculations in Figures 7–9 assume the HCM is carrying 420 kg of fuel, which represents a 75% increase over the dry mass of the X-51A vehicle and would increase the volume of the vehicle by 50%. Larger increases in fuel mass would likely require a different model for the HCM vehicle, so extending the analysis would require a different set of HCM parameters.

The average speeds (excluding boost phase) of the HCMs for the longest-range trajectories in Figures 7–9 are Mach 4.7, 4.9, and 4.9, respectively. The corresponding average speeds for the longest-range MaRV trajectories in those figures are Mach 7.6, 8.2, and 8.5. Moreover, the speed of the MaRV during reentry would be large enough to evade current terminal missile defenses.

The figures show that the range of the HCM for a total mass of 2,300 kg is greatest in the Mach 5 case—about 1,030 km—since the booster can accelerate more fuel to this lower initial speed. This HCM range for $M_{tot} = 2,300$ kg falls to about 960 km for $V_H = \text{Mach } 6$, and 940 km for Mach 6.5. This illustrates that the range depends more on the amount of fuel the vehicle carries than on its initial speed.

As noted, HCMs have a range advantage over BGVs with the same total mass in the cases we considered.

Longer HCM ranges

Operation of the scramjet limits the speed of HCMs during the powered phase to less than about Mach 7. Increasing the distance they can travel within the atmosphere therefore requires increasing the time that the scramjet operates, which requires increasing the amount of fuel the HCM carries.

We can illustrate the limits on an HCM's powered range R_p and show how it depends on the key parameters using the Breguet equation, which

as noted above is an approximate expression for the range of an HCM during its powered phase. It can be written in the form:

$$R_p = \frac{L}{D} \frac{V}{\lambda} I_{sp} \ln \left(1 + \frac{m_f}{M_0} \right) \quad (38)$$

where m_f is the fuel mass and M_0 is the mass of the vehicle without fuel. This equation assumes that the vehicle is traveling with constant speed V and constant L/D .⁹¹

Since specific impulse for a scramjet falls off with $1/V$, it is convenient to write it as:

$$I_{sp}(V) = \frac{I_{sp}^{(s)} V^{(s)}}{V} \quad (39)$$

where $I_{sp}^{(s)}$ is the value of the specific impulse at a speed $V^{(s)}$.⁹² Equation 38 can then be written:

$$R_p = \left(\frac{L}{D} \frac{I_{sp}^{(s)} V^{(s)}}{\lambda} \right) \ln \left(1 + \frac{m_f}{M_0} \right) \quad (40)$$

Here, the speed of the vehicle only enters through λ .

The second factor in Equation 40 vanishes for $m_f = 0$ and increases slowly with m_f taking the value 0.7 for $m_f = M_0$, i.e., when the vehicle carries a fuel mass equal to its dry mass. The term in brackets therefore sets the scale of the range of the powered phase. For speeds considered here, $\lambda \sim 0.96$ and varies slowly with velocity, so the range is set by the values of the specific impulse and L/D .

In the calculation above we assumed a vehicle with $I_{sp}^{(s)} = 900$ s at $V^{(s)} = \text{Mach } 5$ and $L/D = 1.3$ to 1.5 during the powered phase, when the angle of attack is kept low. Using these values, the first term in brackets is about 2,000 km. This value cannot be increased significantly without significant increases in specific impulse or L/D .

These values give a powered range $R_p = 810$ km if the vehicle carries half its mass in fuel ($m_f/M_0 = 0.5$) and 1,400 km if it is able to carry a fuel mass equal to the empty vehicle mass ($m_f/M_0 = 1$). Extending the range to 2,000 km would require an X-51A-like vehicle to carry more than a ton of fuel, which would almost certainly require a redesigned vehicle with a larger vehicle mass, reflecting the need for more structural support to carry this mass of fuel.

As a result, achieving very long powered ranges with HCMs appears difficult—even if there is not a limit on total mass as there is for

air-launched vehicles. This is a general result, applying also to vehicles that are dissimilar to the X-51A.

Note that using hydrogen rather than hydrocarbon fuel will increase the specific impulse by a factor of about three, but the fuel mass m_f that a vehicle could carry would be reduced because hydrogen has a much lower density than hydrocarbons (the density of hydrogen even as a liquid is less than one-tenth that of jet fuel), and storing hydrogen at high pressures and/or low temperatures increases the mass of storage tanks and therefore increases M_0 . As a result, even though hydrogen releases almost three times as much energy per mass in combustion as hydrocarbon fuels, [Equation 40](#) shows that achieving large values of R_p remains difficult.⁹³

Conclusions

The goal of this analysis is to assess the capability of scramjet-powered HCMs and compare them to alternative systems.

HCMs being developed for military use have two major shortcomings. The first is that they are restricted to low hypersonic speeds because of the properties of hydrocarbon fuels. Their low speed means they cannot evade terminal missile defenses similar in capabilities to PAC-3 interceptors.⁹⁴ It also increases their delivery time over a given range compared to other missiles.

The second issue is that increasing the distance an HCM can travel in the atmosphere requires increasing the amount of fuel it carries, which drives up its mass. Adding the mass of the booster needed to accelerate the vehicle up to speed will give a total mass more than double that of the fueled vehicle, so longer range systems may be too massive to be air-launched. In particular, HCMs with ranges longer than 1,100–1,300 km would likely need to be launched from ships or ground-based systems, even with moderate advancements in technology (e.g., improved specific impulse of the scramjet).

Our analysis considers HCMs that use technology more advanced than that of the X-51A, for example, [Figures 4](#) and [7–9](#) assume $I_{sp} = 900$ s rather than 800 s. We also assume the HCM vehicle can carry three and a half times as much fuel as the X-51A without requiring significant increases in structural mass or heat shielding beyond that required to scale up the vehicle to hold the additional fuel. Achieving significantly longer ranges for the same total mass would therefore require further increases in I_{sp} , which may be difficult.

The capabilities shown in [Figure 7](#), therefore, appear to be essentially an upper limit to the capabilities of an HCM that is light enough to be air-launched from fighter aircraft.

In summary, the analysis finds:

- While the total mass (mass of booster+vehicle) of HCMs can be less than BGVs of the same range, MaRVs could be significantly less massive than HCMs of the same range.
- Keeping the mass of HCMs low restricts them to relatively short ranges, since the amount of fuel required for longer ranges drives up their mass.
- HCMs are limited to low hypersonic speeds relative to BGVs and MaRVs (below about Mach 7) because of the properties of hydrocarbon-fueled scramjet engines. Hydrogen-fuel scramjet engines could operate at higher speeds (above Mach 10), but issues of fuel storage limit their utility for military missions.
- HCMs' lower speed gives them longer flight times than BGVs and MaRVs over the same range.
- HCMs' low speeds make them vulnerable to interception by terminal missile defenses, which BGVs and MaRVs can evade.

In addition to strike missions, the other mission discussed for HCMs is carrying sensors and flying low-altitude trajectories to provide surveillance and intelligence-gathering on demand. This mission makes use of the fact that HCMs can maneuver throughout flight, and that their maneuverability is greater than that of BGVs of the same range. However, the difference in maneuverability is due largely to the fact that HCMs travel at lower speeds than BGVs so that smaller forces are needed to turn them.

This finding means, however, that maneuverability can be further increased by further reducing the speed of the vehicle, using supersonic vehicles with speeds of Mach 3 to 4 rather than hypersonic vehicles with speeds of Mach 5 to 6. Supersonic cruise missiles would have several important advantages for applications in which speed is not the primary consideration. Not only would they be more maneuverable than HCMs, they can also be powered by ramjets or turbojets rather than scramjets, which increases their reliability and fuel efficiency. Ramjets and turbojets (like that flown on the SR-71) could have specific impulses more than twice that of a scramjet at Mach 5, leading to more efficient fuel use that could be used to reduce their mass or increase their range.⁹⁵ In addition, since drag scales as V^2 and heating as V^3 , subsonic vehicles face fewer of the structural and thermal problems that can affect hypersonic weapons.

As a result, while there may be specialized missions for which the combination of characteristics of an HCM appear well suited, HCMs do not appear to offer general advantages for either strike or surveillance missions compared to alternative systems. In particular:

- If the priority is low mass for a given range, an HCM performs better than a BGV, but a MaRV performs better than an HCM in

the cases considered here, especially taking into account that MaRV vehicles can likely be made significantly lighter than those considered here.

- If the priority is speed and delivery time, a MaRV performs considerably better than an HCM. Because a MaRV vehicle can be lighter than an HCM vehicle and the fuel it carries, a MaRV can be accelerated to a higher speed with the same total mass of vehicle plus booster.
- Since MaRV vehicles can be made lighter than HCMs, MaRVs could carry a significantly larger warhead.
- Hydrocarbon-fueled HCMs are limited to low hypersonic speeds (below about Mach 7) and are therefore too slow to evade current terminal missile defenses. Both MaRVs and BGVs can have speeds high enough to evade those defenses.
- If the priority is maneuverability during midcourse, then supersonic cruise missiles could have greater maneuverability than HCMs and would allow the system to use a ramjet or turbojet engine, which would be more efficient and reliable than a scramjet. An HCM can maneuver faster and with fewer costs than a BGV. MaRVs cannot maneuver in midcourse.
- If the primary goals for maneuvering are achieving high accuracy and retargeting over hundreds of kms, then a MaRV can do that as well by maneuvering during reentry. The ability to maneuver during midcourse may be less useful for strike weapons that are air-launched because of flexibility in the location of their launch point.
- MaRVs could use the same kinds of sensors and guidance technology being developed for BGVs and HCMs and could therefore have similar accuracy.

The Air Force has expressed interest in HCMs as strike weapons that can be carried on aircraft other than B-52s. Our analysis shows there are better alternatives.

Recent reports say the U.S. Air Force is rethinking its HCM development programs and the role of such weapons. For example, funding for the Air Force's Mayhem program, which was the next step in developing HCMs beyond systems like HACM, has been cut and the Air Force is "conducting an Analysis of Alternatives...over the next year to refine the requirement for high-speed strike." Referring to the Mayhem program, an Air Force official stated, "What we are more interested in right now, in terms of a feasibility perspective, is a high-Mach turbine engine."⁹⁶

Our analysis illustrates some of the key issues that should be considered in assessing the capabilities and desirability of HCMs.

Disclosure statement

No potential conflict of interest was reported by the author(s).

ORCID

Cameron L. Tracy  <http://orcid.org/0000-0002-0679-8522>

Notes

1. The term “glide” refers to the unpowered flight of the vehicle in the atmosphere while it is being held aloft by lift forces and does not refer to the unpowered ballistic phase after booster burnout.
2. Cameron L. Tracy and David Wright, “Modelling the Performance of Hypersonic Boost-Glide Missiles,” *Science and Global Security* 28 (2021). <http://scienceandglobalsecurity.org/archive/sgs28tracy.pdf>; David Wright and Cameron L. Tracy, “Hypersonic Weapons: Vulnerability to Missile Defenses and Comparison to MaRVs,” *Science & Global Security* 31, 3 (2023), <https://scienceandglobalsecurity.org/archive/sgs31wright.pdf>.
3. See, for example, Michael Morrow, “Air Force Moves Out on Hypersonic Cruise Missile Flight Testing in FY25,” *Breaking Defense*, <https://breakingdefense.com/2024/03/air-force-moves-out-on-hypersonic-cruise-missile-flight-testing-in-fy25/> (accessed March 14, 2024); John A. Tirpak, “Kendall: Air Force ‘More Committed’ to HACM After Latest Unsuccessful ARRW Test,” *Air and Space Forces*, <https://www.airandspaceforces.com/kendall-air-force-hacm-unsuccessful-arrw-test/> (accessed March 28, 2023); Jon Harper, “Air Force has ‘concerns’ about HACM; hasn’t ruled out boost-glide hypersonic weapons,” *Defensescoop*, <https://defensescoop.com/2023/12/21/air-force-hypersonic-weapons-arrw-hacm/> (accessed December 12, 2023).
4. Kelley M. Sayler, “Hypersonic Weapons: Background and Issues for Congress,” Congressional Research Service R45811, <https://crsreports.congress.gov/product/pdf/R/R45811> (accessed February 9, 2024).
5. Jon Harper, “Navy’s Future HALO ‘Hypersonic’ Missile Might not Actually be Hypersonic,” *Defensescoop*, <https://defensescoop.com/2023/04/03/navys-future-halo-hypersonic-missile-might-not-actually-be-hypersonic/> (accessed April 3, 2023).
6. Brigadier General Charles R. Davis, “F-35 Program Brief,” https://web.archive.org/web/20200725033118/https://www.jsf.mil/downloads/documents/AFA_Conf_-_JSF_Program_Brief_-_26_Sept_06.pdf (accessed September 26, 2006).
7. John A. Tirpak, “‘Mayhem’ Will Be Larger, Multi-Role Air-Breathing Hypersonic System for USAF,” *Air and Space Forces Magazine*, <https://www.airandspaceforces.com/mayhem-will-be-larger-multi-role-air-breathing-hypersonic-system-for-usaf/> (accessed August 19, 2020); John A. Tirpak, “New Boeing Pylon Could Shift Hypersonics Testing to B-1, Add Bomb Capacity,” *Air and Space Forces Magazine*, <https://www.airandspaceforces.com/new-boeing-pylon-b-1/> (accessed May 19, 2023).
8. Steve Trimble, “More ARRW Details Emerge as Congress, White House Add New Hurdles,” *Aviation Week and Space Technology*, <https://aviationweek.com/defense-space/missile-defense-weapons/more-arrw-details-emerge-congress-white-house-add-new-hurdles> (accessed July 14, 2021).
9. Congressional Budget Office, “U.S. Hypersonic Weapons and Alternatives,” <https://www.cbo.gov/system/files/2023-01/58255-hypersonic.pdf> (accessed January 2023).

10. Jon Harper, “Air Force has ‘Concerns’”; Stephen Losey, “US Air Force drops Lockheed hypersonic missile after failed tests,” *Defense News*, <https://www.defensenews.com/air/2023/03/30/us-air-force-drops-lockheed-hypersonic-missile-after-failed-tests/> (accessed March 30, 2023); Stephen Losey, “Air Force Budget Backs Raytheon Hypersonic, No Lockheed Missile Funds,” *Defense News*, <https://www.defensenews.com/air/2024/03/12/air-force-budget-backs-raytheon-hypersonic-no-lockheed-missile-funds/> (accessed March 12, 2024).
11. Joseph Trevithick, “Hypersonic Strike Aircraft Capability is Part of The Air Force’s Shadowy Project Mayhem, *The War Zone*, <https://www.twz.com/43545/hypersonic-strike-aircraft-capability-is-part-of-air-forces-shadowy-project-mayhem> (accessed December 20, 2021).
12. John Tirpak, “‘Mayhem’ Will Be Larger, Multi-Role Air-Breathing Hypersonic System for USAF,” *Air and Space Forces*, <https://www.airandspaceforces.com/mayhem-will-be-larger-multi-role-air-breathing-hypersonic-system-for-usaf/> (accessed August 19, 2020).
13. Howard Altman and Joseph Trevithick, “Future of Mayhem Hypersonic Strike-Recon Aircraft Program Murky,” *The Warzone*, <https://www.twz.com/news-features/future-of-mayhem-hypersonic-strike-recon-aircraft-program-murky> (accessed February 16, 2024).
14. Sidharth Kaushal, “The Zircon: How Much of a Threat Does Russia’s Hypersonic Missile Pose?” Royal United Services Institute (RUSI) paper, <https://www.rusi.org/explore-our-research/publications/commentary/zircon-how-much-threat-does-russias-hypersonic-missile-pose> (accessed January 24, 2023).
15. Thomas d’Istria, “War in Ukraine: Russia Steps Up Strikes on Kyiv’s Energy Infrastructure,” *Le Monde*, https://www.lemonde.fr/en/international/article/2024/03/26/war-in-ukraine-russia-steps-up-strikes-on-kyiv-s-energy-infrastructure_6657030_4.html (accessed March 26, 2024).
16. Paul Bernstein and Dain Hancock, “China’s Hypersonic Weapons,” *Georgetown Journal of International Affairs*, <https://gjia.georgetown.edu/2021/01/27/chinas-hypersonic-weapons/> (accessed January 27, 2021).
17. For a single-stage booster, this scaling is exact, due to the rocket equation.
18. Wright and Tracy, “Hypersonic Weapons.”
19. See, for example, Joseph Trevithick, “Here’s How Hypersonic Weapons Could Completely Change the Face of Warfare,” *The War Zone*, <https://www.thedrive.com/the-war-zone/11177/heres-how-hypersonic-weapons-could-completely-change-the-face-of-warfare> (accessed June 6, 2017); “Hypersonic Strike and Defense: A Conversation with Mike White,” *Center for Strategic and International Studies*, <https://www.csis.org/analysis/hypersonic-strike-and-defense-conversation-mike-white> (accessed June 10, 2021).
20. Dora Musielak, *Scramjet Propulsion: A Practical Introduction* (Hoboken, NJ: John Wiley & Sons, 2023), 8.
21. Air Force Materiel Command, “X-51A Waverider,” <https://www.afmc.af.mil/News/Article-Display/Article/154198/x-51-waverider-makes-historic-hypersonic-flight/>.
22. Paul J. Ortwerth, “Scramjet Flowpath Integration,” Chapter 17, in *Scramjet Propulsion*, E.T. Curran and S.N.B. Murthy, eds., American Institute of Aeronautics and Astronautics (AIAA), Progress in Aeronautics and Astronautics Vol. 198, 2000.
23. Musielak, *Scramjet Propulsion*; Kevin G. Bowcutt, “Physics Drivers of Hypersonic Vehicle Design,” AIAA Space Forum, 22nd AIAA International Space Planes and Hypersonic Systems and Technologies Conference, 17–19 September 2018, Orlando, Florida.



24. Musielak, *Scramjet Propulsion*, Chap. 11.
25. U.S. Airforce, “X-51A Waverider,” <https://www.af.mil/About-Us/Fact-Sheets/Display/Article/104467/x-51a-waverider/>.
26. Musielak, *Scramjet Propulsion*, 24–26, 444–448; Laurie A. Marshall, Griffin P. Corpening, and Robert Sherrill, “A Chief Engineer’s View of the NASA X-43A Scramjet Flight Test,” AIAA/CIRA 13th International Space Planes and Hypersonics Systems and Technologies, AIAA 2005–3332; Laurie A. Marshall, Catherine Bahm, Griffin P. Corpening, and Robert Sherrill, “Overview with Results and Lessons Learned of the X-43A Mach 10 Flight,” AIAA/CIRA 13th International Space Planes and Hypersonics Systems and Technologies, AIAA 2005–3336; Eugene A. Morelli, Stephen D. Derry, and Mark S. Smith, “Aerodynamic Parameter Estimation for the X-43A (Hyper-X) from Flight Data,” AIAA Atmospheric Flight Mechanics Conference and Exhibit, 15–18 August 2005, San Francisco, California, AIAA 2005–5921; Charles R. McClinton, “X-43–Scramjet Power Breaks the Hypersonic Barrier,” Dryden Lectureship in Research for 2006, 44th AIAA Aerospace Sciences Meeting and Exhibit 9–12 January 2006, Reno, Nevada, AIAA 2006–1.
27. Joseph M. Hank, James S. Murphy, and Richard C. Mutzman, “The X-51A Scramjet Engine Flight Demonstration Program,” 15th AIAA International Space Planes and Hypersonic Systems and Technologies Conference, 28 April–1 May 2008, Dayton, Ohio, AIAA 2008–2540.
28. Mark Lewis, “X-51 scams into the future,” *Aerospace America*, October 2010, 26.
29. Guy Norris, “High-Speed Strike Weapon to Build on X-51 Flight, *Aviation Week and Space Technology*, https://web.archive.org/web/20140104023933/http://www.aviationweek.com/Article/PrintArticle.aspx?id=/article-xml/AW_05_20_2013_p24-579062.xml&p=1&printView=true (accessed May 20, 2013).
30. John A. Tirpak, “New HAWC Hypersonic Missile Sets Record for Endurance,” Air and Space Forces, <https://www.airandspaceforces.com/new-hawc-hypersonic-missile-sets-record-for-endurance/> (accessed April 6, 2022).
31. Mikayla Easley, “DARPA Taps Raytheon for Next Phase of Air-Breathing Hypersonic Program,” *Defensescoop*, <https://defensescoop.com/2023/07/17/raytheon-darpa-mohawc-contract/> (accessed July 16, 2023).
32. Congressional Budget Office, “U.S. Hypersonic Weapons.”
33. Our calculations of density and sound speed use the 1976 Standard Atmosphere calculator, <https://www.digidutch.com/atmoscalc/index.htm>, which shows that Mach 1 = 295.070 m/s for all altitudes relevant to the X-51A test (11 to ~21 km).
34. Norris, “High-Speed Strike Weapon.”
35. Christopher M. Rondeau and Timothy R. Jorris, “X-51A Scramjet Demonstrator Program: Waverider Ground and Flight Test,” SFTF 44th International/SETP Southwest Flight Test Symposium, 28 Oct–1 Nov 2013, Ft Worth, Texas; Musielak, *Scramjet Propulsion*; US Air Force, “X-51A Waverider.”
36. “Robert J. Collier Trophy Nominee: X-51A WaveRider” Presentation, slides and transcript, 2014, <https://slideplayer.com/slide/4217801/>.
37. Norris, “High-Speed Strike Weapon.”
38. Collier Trophy Nominee; Kevin G. Bowcutt, “Tackling the Extreme Challenges of Air-Breathing Hypersonic Vehicle Design, Technology, and Flight,” Slides from Mathematics, Computing & Design Symposium Honoring Antony Jameson’s 80th Birthday, Stanford University, CA, <http://aero-comlab.stanford.edu/jameson/aj80th/bowcutt.pdf> (accessed November 21, 2014); Norris, “High-Speed Strike Weapon.”
39. Rondeau and Jorris, “X-51A Scramjet Demonstrator Program.”
40. Rondeau and Jorris, “X-51A Scramjet Demonstrator Program.”

41. Bowcutt, "Tackling the Extreme Challenges."
42. Norris, "High-Speed Strike Weapon."
43. The reference area is a measure of the surface area of the vehicle used to calculate aerodynamic quantities. By explicitly reflecting the size of the object, it allows the coefficients C_L and C_D to depend on the shape of the object and not its size. Selection of the reference area is essentially arbitrary (e.g., use of the cross-sectional area in a given projection versus use of the planform area of a wing), but it is important when comparing values of non-dimensional coefficients to use consistently defined reference areas. See John Anderson, *Fundamentals of Aerodynamics*, 6th ed. (New York: McGraw-Hill Education, 2017), 24–25, 32; David Mostaza Prieto, Benjamin P. Graziano, and Peter C.E. Roberts, "Spacecraft drag modelling," *Progress in Aerospace Sciences* 64 (2014).
44. Musielak, *Scramjet Propulsion*, 48.
45. Musielak, *Scramjet Propulsion*, 46–47.
46. Keeping α constant and instead changing the lift by reducing q_0 to compensate for the change in fuel mass would require nearly a 20% decrease in q_0 , and therefore in thrust, when burning 120 kg of fuel, and a considerably larger decrease for some of the variations we consider below.
47. Bowcutt, "Tackling the Extreme Challenges."
48. James E. Walker, "Engine Requirements for Supersonic Flight," Chapter 3, in *Ramjet Technology* (Silver Spring, MD: The Johns Hopkins University Applied Physics Laboratory, 1952), <https://apps.dtic.mil/sti/tr/pdf/AD0041745.pdf>. In discussing supersonic vehicles, Walker notes that for low-altitude supersonic flight "a fraction of one degree frequently provides adequate lift to support a typical missile. This fact is a consequence of the extremely large dynamic pressures..."
49. Bowcutt, "Physics Drivers."
50. Marshall, Corpening, and Sherrill, "A Chief Engineer's View;" Marshall, Bahm, Corpening, and Sherrill, "Overview with Results and Lessons Learned."
51. Anderson, *Fundamentals of Aerodynamics* (6th Edition), Chap. 5; Frank J. Regan and Satya M. Anandakrishnan, *Dynamics of Atmospheric Re-Entry* (Washington, DC: AIAA, 1993), Chap. 9.
52. Eq. 9 gives minimum drag at $\alpha=0$. In general, this may not be true for an asymmetric body; several studies show the minimum for vehicles similar to the X-51A at angles of attack of a couple degrees (Kevin G. Bowcutt, "Multidisciplinary Optimization of Airbreathing Hypersonic Vehicles," *Journal of Propulsion and Power*, 17:6, November–December 2001; Yan-dan Deng, Sheng-hong Huang, Ji-ming Yang, and Di Cheng, "A Preliminary Investigation on Aerodynamic Characteristics of an X-51A-like Aircraft Model," *Acta Aerodynamica Sinica*, 2013 (In Chinese)). Shifting the position of the minimum can reduce slightly the drag for angles-of-attack at which the vehicle is flown during powered flight. Doing so gives additional parameters to adjust the shape of the lift, drag, and L/D curves, but our results are not sensitive to this value, so for simplicity we assume it is zero. Moreover, animations show the X-51A vehicle flying upside down for part of its powered flight; this inversion symmetry suggests that the minimum of both lift and drag occurs near $\alpha = 0$ ("Hypersonic Waverider How the USAF X-51A Scramjet Works," Video, Space.com, 2013, <https://www.youtube.com/watch?v=UxwMNWrvttU>).
53. The specific impulse of an air-breathing engine is defined in terms of the fuel mass flow, rather than the fuel and oxidizer mass flow, as it would be for a rocket engine.
54. Ortwerth, "Scramjet Flowpath Integration;" Musielak, *Scramjet Propulsion*.



55. Craig Covault, “X-51 scramjet flights poised to bridge air and space propulsion for space launch, Prompt Global Strike, *Spaceflight Now*, 16 May 2010, <https://spaceflightnow.com/news/n1005/16waverider/>; Air Force Materiel Command, “X-51A Waverider.”
56. See, eg, Musielak, *Scramjet Propulsion*, Fig. 1.8.
57. Marshall, Corpener, and Sherrill, “A Chief Engineer’s View of the NASA X-43A Scramjet Flight Test,” Christopher D. Karlgaard, Paul V. Tartabiniy, Robert C. Blanchardz, Michael Kirschx, and Matthew D. Toniolo, “Hyper-X Post-Flight Trajectory Reconstruction,” AIAA 2004-4829, AIAA Atmospheric Flight Mechanics Conference and Exhibit, Providence, RI, 16–19 August 2004; Christopher D. Karlgaard, John G. Martiny, Paul V. Tartabiniz, Mark N. Thornblomx, “Hyper-X Mach 10 Trajectory Reconstruction,” AIAA 2005-5920, AIAA Atmospheric Flight Mechanics Conference and Exhibit, San Francisco, CA, 15–18 August 2005.
58. Rondeau and Jorris, “X-51A Scramjet Demonstrator Program.”
59. Plots of the glide trajectories in the X-43A tests supports this assumption; see Karlgaard et al., “Hyper-X Post-Flight Trajectory” and Karlgaard et al., “Hyper-X Mach 10 Trajectory.”
60. These calculations use the methods described in Tracy and Wright, “Modelling the Performance.”
61. These values are consistent with the values of the lift and drag coefficients resulting from the values of D_0 and D_2 found in the fitting process below. The range and time of glide are calculated numerically assuming a standard atmosphere, since analytic range equations are less accurate for glides at very low altitudes.
62. $L/D=1.8$ also seems to be roughly consistent with other descriptions of the flight time, although these descriptions are more ambiguous. For example, Bowcutt, “Tackling the Extreme Challenges,” says that the scramjet operated for 209 s, that there were 361 s of “controlled flight,” and that the vehicle traveled about 240 nm (444 km) in six minutes. This appears consistent with the estimate of $L/D=1.8$, if we assume “controlled flight” ended near the time that the vehicle slowed to Mach 3 (885 m/s). Note that Rondeau and Jorris, “X-51A Scramjet Demonstrator Program,” said that PID maneuvers “were to be performed at Mach numbers 5, 4, 3, and 2,” suggesting that not all of them were completed. In this case, glide with $L/D=1.8$ would have a range of 157 km in 135 s ($135\text{ s} = 361 - 226$, where 226 s is an estimate of the time between end of boost and end of powered flight, which includes a short coast phase, scramjet start, and scramjet burn). This would give a total range of $157 + 325 = 482$ km (where 325 is an estimate of the range to the end of powered flight starting at the end of boost).
63. See, for example, Figure 6 in Hank, Murphy, and Mutzman, “The X-51A Scramjet.”
64. The X-51A vehicle traveled about 25 km while the rocket booster was burning. The distance traveled during boost by the BGV and MaRV vehicles considered in the final section may be somewhat longer than this since the booster burnout speed is higher and the burn time is longer in those cases.
65. Bowcutt, “Physics Drivers.”
66. Wright and Tracy, “Hypersonic Weapons.”
67. Wright and Tracy, “Hypersonic Weapons.”
68. Steve Fetter, “A Ballistic Missile Primer,” 1990, <https://fetter.it-prod-webhosting.aws.umd.edu/sites/default/files/fetter/files/1990-MissilePrimer.pdf>. Note we are using a different definition of the fuel fraction factor φ .
69. For air-launched vehicles, the launch platform will typically have a speed of about Mach 0.8. Numerical estimates show that the drag and gravity losses from these

- launches would also be about Mach 0.8, so we assume here that the two contributions offset each other.
70. For this calculation, we assume that the both the speed at booster burnout and at the start of the scramjet burn are Mach 6.5.
 71. Tirpak, "New HAWC Hypersonic Missile."
 72. *L/D* of the X-43A can be estimated from the trajectory information in Marshall, Corpenering, and Sherrill, "A Chief Engineer's View;" Marshall, Bahm, Corpenering, and Sherrill, "Overview with Results and Lessons Learned."
 73. Wright and Tracy, "Hypersonic Weapons."
 74. Wright and Tracy, "Hypersonic Weapons."
 75. "Hypersonic Strike and Defense: A Conversation with Mike White."
 76. Wright and Tracy, "Hypersonic Weapons."
 77. The ratio of densities at these altitudes is approximately $\exp(\Delta h/6.7)$, where Δh is the change in altitude in kilometers.
 78. Wright and Tracy, "Hypersonic Weapons."
 79. These two cases for the HCM correspond to bank angles of 28° and 45°, respectively.
 80. W.J.A. Dahm, "Innovation in Aeronautical and Exo-Atmospheric Propulsion," August 2009, AIAA Joint Propulsion Conference 2009, Denver, Colorado, <http://dx.doi.org/10.13140/RG.2.1.2482.1361>.
 81. This process is described in detail in Wright and Tracy, "Hypersonic Weapons," which discusses how BGV range is calculated.
 82. Wright and Tracy, "Hypersonic Weapons."
 83. Wright and Tracy, "Hypersonic Weapons."
 84. In Figure 8, the loft angle γ varies between 25° for the smallest mass to zero for the largest mass. For Figure 9, γ varies between 35° and 10°, and for Figure 10, γ varies between 40° and 20°.
 85. Wright and Tracy, "Hypersonic Weapons."
 86. Tirpak, "'Mayhem' Will Be Larger."
 87. These calculations are detailed in Wright and Tracy, "Hypersonic Weapons."
 88. Wright and Tracy, "Hypersonic Weapons."
 89. Amy Woolf, *Conventional Prompt Global Strike and Long-Range Ballistic Missiles: Background and Issues* (Washington, DC: Congressional Research Service, 2021), <https://crsreports.congress.gov/product/pdf/R/R41464>; National Research Council, U.S. *Conventional Prompt Global Strike: Issues for 2008 and Beyond*, Committee on Conventional Prompt Global Strike Capability (2008): 206–215, <https://doi.org/10.17226/12061>.
 90. The mass of the CTM MaRV is given in Table 4.1 in National Research Council, U.S. *Conventional Prompt Global Strike*.
 91. Bowcutt, "Physics Drivers."
 92. Ortwerth, "Scramjet Flowpath Integration;" Musielak, *Scramjet Propulsion*.
 93. Because of its higher speed, a hydrogen-fueled HCM could have a significantly longer glide range than a hydrocarbon-fuel vehicle.
 94. Note that some sources quote very short radar detection ranges (tens of kilometers) for HCMs, which could help them evade defenses (Kaushal, "The Zircon"). However, such detection ranges apparently assume that HCMs can fly at very low altitudes typical of subsonic cruise missiles, less than 100 meters, which they cannot. HCMs fly at altitudes of 20 to 30 km, and dropping to such low altitudes would require them to fly at much slower speeds to reduce the stress and heating on the vehicle and would then require an engine other than a scramjet, which could not operate

- at those speeds. An HCM flying at an altitude of about 20 km could likely be detected by a ground or ship-based radar at a range of several hundred kilometers.
95. Nathan Meier, "Military Turbojet/Turbofan Specifications," <https://www.jet-engine.net/miltfspec.htm> (accessed September 3, 2021).
 96. Altman and Trevithick, "Future of Mayhem."
 97. This version of the range equation is a good approximation for these speeds. A more exact equation is given in Wright and Tracy, "Hypersonic Weapons," along with a derivation of both equations.
 98. The US HTV-2 test BGV reportedly flew with $\alpha = 10\text{--}15$ degrees. The X-43A flew with $\alpha = 1\text{--}2.5$ degrees.
 99. Wright and Tracy, "Hypersonic Weapons."
 100. Ortwerth, "Scramjet Flowpath Integration," says that if you want to keep L/D constant at an optimum value, you can vary the altitude of flight. That will change q_0 , which doesn't seem to be what was done for the X-51A, the range of q_0 reported for the flights was too small to counter the change in mass and keep L/D constant. This is obviously easier for H-fueled HCMs since the change in mass is very small.
 101. For JP-7 fuel, $f=0.0664$ so by far most of the mass being accelerated is that of air rather than fuel.
 102. Eq. A10 for thrust assumes that the vehicle is designed to capture sufficient airflow for the engine to burn the fuel flowing at a rate m_f at the speeds it is designed to fly; that required air flow is given by Eq. A12.
 103. Musielak, *Scramjet Propulsion*, 46–47.

Appendix A. Basic hypersonic flight equations

A key parameter in the analysis of hypersonic vehicles is dynamic pressure, q_0 , which characterizes the kinetic energy per unit volume of the air surrounding a vehicle. This quantity is defined by:

$$q_0 = \frac{1}{2} \rho V^2 \quad (\text{A1})$$

where ρ and V are the atmospheric density and speed at which the vehicle is flying, respectively. We consider below how q_0 enters into the design and flight of boost-glide vehicles (BGVs) and hypersonic cruise missiles (HCMs).

BGV analysis

BGVs are boosted to high speed by rockets, then glide without power. The key equations characterizing the forces acting on these vehicles during glide (lift, gravity, drag, and the stresses experienced by vehicle structures) and their surface heating are:

$$F_{\text{Lift}} = C_L A q_0 = Mg\lambda \quad (\text{A2})$$

$$F_{\text{Drag}} = C_D A q_0 \quad (\text{A3})$$

$$\text{Physical stress} \sim \rho V^2 \sim q_0 \quad (\text{A4})$$

$$\text{Heating} \sim \rho V^3 \sim q_0 V \quad (\text{A5})$$

where C_L and C_D are the lift and drag coefficients and A is a reference area. The second equality of [Equation A2](#) represents the requirement that the lift be sufficient to counter gravity and keep the vehicle aloft. Here $g = 9.8 \text{ m/s}^2$ and:

$$\lambda(V) = 1 - \frac{V^2}{V_e^2} \quad (A6)$$

is an inertial term that reduces the apparent gravitational force due to the high speed of the vehicle, where $V_e = [g(R_e + h)]^{1/2} \approx 7,915 \text{ m/s}$ at altitudes relevant here; V_e is the orbital velocity of an object in a circular orbit at altitude h . $\lambda(V)$ varies slowly with V in the range of speeds considered here, from 0.966 at Mach 5 to 0.933 at Mach 7.

The glide range of a BGV for the speeds considered here can be written:

$$R_{\text{glide}} = \frac{L}{D} \frac{V^2 - V_f^2}{2g\lambda(V)} \quad (A7)$$

where V is the speed at the start of glide, the lift-to-drag ratio is $L/D = F_{\text{lift}}/F_{\text{drag}} = C_L/C_D$, and V_f is the speed at the end of glide phase. To calculate the range over which the vehicle could remain in hypersonic flight, $V_f = \text{Mach } 5$.⁹⁷

Both C_L and C_D , and therefore L/D , are functions of the angle-of-attack α at which the vehicle is flown.⁹⁸

BGVs are designed to have a value of L/D that is as large as possible, since it determines the range for a given speed V , as shown by [Equation A7](#). Yet while subsonic aircraft can have L/D of 15 to 20, the BGVs the United States have flight tested appear to have values less than three.⁹⁹

Using [Equation A2](#), the dynamic pressure can be written as:

$$q_0 = \frac{Mg\lambda}{C_L A} = \frac{\beta g \lambda}{L/D} \quad (A8)$$

where the ballistic coefficient $\beta = M/C_D A$. The BGV's equilibrium flight altitude h can be found from the atmospheric density $\rho(h)$ during flight:

$$\rho(h) = \frac{2Mg\lambda}{C_L A V^2} = \frac{2q_0}{V^2} \quad (A9)$$

The value of q_0 during BGV flight is not highly constrained. The vehicle must be flown with q_0 low enough to produce stress and heating ([Equations A4](#) and [A5](#)) that the vehicle can withstand at its flight speed V , but high enough to produce lift sufficient to keep the vehicle aloft ([Equation A2](#)) at the angle of attack that maximizes L/D . The vehicle will then glide at an altitude determined by those values of q_0 and V ([Equation A9](#)).

HCM analysis

The situation for HCMs is different from that of BGVs because these vehicles must also take in enough air from the atmosphere to burn fuel in the engine at a level that produces high thrust. Unlike rocket engines, which carry both their fuel and oxidizer, HCMs carry fuel but get their oxidizer from the atmosphere.

The mass of the HCM will change as it burns its fuel. Since q_0 is kept roughly constant during flight, [Equation A2](#) implies that $C_L A$ will have to decrease during the powered phase, which means the angle-of-attack α will have to change while the scramjet is burning.¹⁰⁰

Adding a scramjet to the vehicle requires several equations describing vehicle thrust, vehicle mass, and airflow rate, in addition to [Equations A2](#) through [A5](#):

$$T = \dot{m}_f g I_{sp} \quad (A10)$$

$$M(t) = M_0 - \dot{m}_f t \quad (A11)$$

$$\dot{m}_a = \frac{\dot{m}_f}{f} = \rho V A_{in} = 2 \frac{A_{in}}{V} q_0 \quad (A12)$$

[Equation A10](#) gives the thrust T of the engine in terms of \dot{m}_f , the fuel flow rate to the engine, and I_{sp} , the engine's specific impulse. [Equation A11](#) gives the change in vehicle mass $M(t)$ as the fuel burns, where t is the time the fuel has been burning and $M_0 = M(0)$. [Equation A12](#) gives the air flow to the engine needed to burn the fuel, where A_{in} is the inlet capture area that the vehicle uses to collect air for the engine, and:

$$f = \frac{\dot{m}_f}{\dot{m}_a} \quad (A13)$$

is the ratio between the mass flows of air and fuel needed to burn the fuel efficiently.

The angle-of-attack α at which the vehicle is flown is determined by [Equation A2](#), which requires that:

$$C_L(\alpha) A = \frac{M(t) g \lambda(V)}{q_0} \quad (A14)$$

At constant q_0 , this angle therefore depends on t (through $M(t)$) and weakly on V (through λ) during the HCM's powered phase.

Because HCMs are flown at high values of q_0 , as discussed below, [Equation A14](#) shows that the vehicle will be flown with a small value of $C_L A$, which corresponds to a small value of α during the powered phase. As a result, an HCM will typically not fly at a value of α that maximizes L/D during this phase.

HCMs and q_0

For HCMs, the value of q_0 is determined by the following considerations.

The thrust generated by an HCM is produced by chemical reactions in the engine that accelerate the mass of the fuel and the air used to burn it to very high speeds; the engine then converts that change in momentum to a change in momentum of the vehicle. Achieving high thrust requires the engine to accelerate a large mass of fuel and air to a high speed, which then exits the vehicle.

High thrust therefore requires a large air mass flow into the engine.¹⁰¹ [Equation A12](#) shows that the air flow is proportional to q_0 , which requires HCMs to fly at high q_0 .¹⁰² This explains in part why the X-51A was flown at very high q_0 , around 110 kPa, compared to the HTV-2 BGV, which flew at q_0 less than 20 kPa.

At the same time, however, the value of q_0 will be limited by the levels of stress and heating the vehicle can withstand, since both scale with q_0 ([Equations A4](#) and [A5](#)).

It is important to note that HCMs rely on active cooling since they circulate their fuel to collect heat from portions of the vehicle surface and engine before it enters the combustor, which both provides cooling and preheats the fuel. This allows HCMs to operate with higher surface heating rates than they could otherwise.

The result of these considerations is that HCMs must fly in a narrow flight corridor defined by suitable combinations of velocity and altitude. If q_0 is too low there will not be enough air mass flow to the engine, but if q_0 is too high the stresses and heating will be too great.¹⁰³ The X-51A was flown keeping q_0 relatively constant during flight, presumably to maintain high thrust and acceptable levels of stress and heating.